ELSEVIER

Catalysis Today 51 (1999) 319–348

CATALYSIS TODAY

Supported metal oxide and other catalysts for ethane conversion: a review

Miguel A. Bañares*

Instituto de Catálisis y Petroleoquímica, CSIC, Campus UAM-Cantoblanco, E-28049, Madrid, Spain

Abstract

The conversion of ethane to ethylene, aromatics, and oxygenates and combustion on supported metal oxide catalysts are discussed. Updated information on the structure and performance of supported oxide catalysts in reactions is offered, underlining the importance of in situ characterization under reaction conditions in order to fully understand the structure and reactivity of supported metal oxide catalysts at molecular level. Support effects, the stability of supported oxide catalysts, molecular structures and oxidation states under reaction conditions, and the effects of metal oxide and additive loading are discussed. The role of terminal and bridging oxygen species is also addressed. Emphasis is placed on the relevance of surface species vs. bulk structure and characterization. A section devoted to new trends in the selective oxidation of ethane to afford high yields and lower working temperatures is included.

Keywords: Ethane conversion; Oxidation; Selectivity; ODH; Oxygenates; Aromatization; Additives; Support effect; Surface coverage; Oxides; Microporous materials

1. Introduction

The heterogeneous catalytic oxidation on oxides is extensively used in catalysis for selective and total oxidation processes. However, the cost and availability of feedstocks can seriously limit the process involving olefins because the raw materials constitute 60–70% of the costs of production. This creates a strong dependence on the raw materials market. Despite the large reserves of alkanes from natural gas or as liquefied petroleum gas (LPG), except for the conversion of butane to maleic anhydride on VPO catalysts [1], no industrial process appears to be operative for the conversion of alkanes. The activation of alkanes is more difficult than that of the corresponding olefins, but their large reserves underline the economic interest in their conversion. The use of olefins and olefin-derived products is steadily increasing and their production is mainly based on steam cracking and FCC processes, which are energy intensive. At the same time, the reserves of raw material for these processes are becoming more and more limited. Consequently, more abundant and economic sources for the production of olefins must be sought. The reactivity of feedstocks determines their ease of conversion. The lower alkanes are the least reactive hydrocarbons, and this has preserved them over time. Also, their low reactivity has hindered their use in industrial processes. Despite this, the increasing costs of traditional feedstocks currently demands advances in the conversion of paraffins. The selective conversion of paraffins

*Tel.: +34-1-5854788; fax: +34-1-5854760; e-mail: mbanares@icp.csic.es

0920-5861/99/$ – see front matter
PII: S0920-5861(99)00053-X

to aromatics, to olefins or to organic molecules containing oxygen or nitrogen atoms is a source of many chemical products. Ethane is the second major component of natural gas, which makes it a potential source of chemicals such as light olefins, oxygenates and aromatic hydrocarbons [2]. The oxidation of lower alkanes is a key issue in the use of natural gas and volatile petroleum fractions as new feedstocks. The oxidation of ethane has been reported to yield ethylene, aromatics and acetaldehyde or acetic acid. Ethylene is mainly used for the production of low density polyethylene (LDPE), high density PE, ethylene dichloride, ethylene oxide, linear LDPE and ethylbenzene, among other compounds. The aromatization of ethane could extend the sources of aromatics and should offer an alternative route for the separation of ethane from methane during the oxidative coupling process –OCM– since its recovery is hard to accomplish [3,4]. The production of aromatics is important owing to their use as a source of petrochemicals and also due to their high octane number. Acetaldehyde has been used for the production of acetic acid, but this process has now been replaced by Monsanto carbonylation of methanol. Acetic acid is mainly used for the production of vinyl acetate, acetic anhydride and solvent esters. The development of direct conversion of ethane to C_2-oxygenate hydrocarbons would provide an attractive alternative. In turn, the processes of combustion eliminate toxic compounds.

Catalysis by oxides is extensively used. The presence of a support is of economic interest and such supports provide new means to tailor catalytic performance by altering the exposure of the sites and modifying their nature by interaction with the support. This review addresses the results reported on the conversion of ethane (partial oxidation, aromatization and combustion) on supported oxides, assessing the relevance of the catalyst formulation (support, active phase, additive), the interaction with the support (specific support and coverage) and the reaction conditions (type of oxidant, gas-phase additives) in a search for a molecular understanding of the structure of the active site and its activity. The transformation of catalyst structure under reaction conditions and its implications in catalytic performance are discussed, underlining the need for the development and routine use of in situ characterization methodologies. A further aim of this review to present new concepts as regards conversion of ethane since some of the most attractive results have come from alternative means of activating ethane.

1.1. Nature of supported oxides

Supported oxides consist of an oxide deposited on the surface of another oxide (support). The supported oxide (M) binds to the support (S) via bridging M–O–S bonds, which are formed in part by reaction with surface hydroxyl groups [5,6]. For instance, surface vanadia species present a terminal V=O bond and three bridging oxygen to the support, or surface molybdena species present a terminal Mo=O bond and four bridging oxygens to the support [7,8]. Similar structures are observed for other supported oxides [9]. Such structures are affected by ambient humidity, which hydrolyzes the M–O–S bond, resulting in an aqueous solution of the supported oxide. The chemistry of these species has been studied by several authors [10–13], although this is not present under ethane oxidation conditions, typically run above 573 K, where the catalyst remains essentially dehydrated. Some changes in the dehydrated structure may occur during the reaction of ethane, however, the structure is related to the dehydrated one [14], as in the case of other alkane oxidation reactions [15–17]. Dehydrated supported oxide species are present as surface isolated or bidimensional polymeric species, and aggregate as crystals above the monolayer coverage. The dehydrated surface dispersed species are stabilized by their interaction with the surface groups of the support (hydroxyls), and the surface population of hydroxyl sites determines the monolayer coverage of the supported oxide. We consider the monolayer coverage as the maximum loading at which the supported oxide is deposited as a surface species, free of tridimensional aggregates. Pure geometric consideration fail to provide correct estimations of the monolayer coverage since the chemical stabilization of the surface species is not considered. For instance, a silica (Cabot, 337 m^2/g) with a much higher surface area than an alumina (Engelhard, 222 m^2/g) reaches monolayer coverage at 12% V_2O_5 (ca. 2 V atoms/nm^2), whereas a loading of 25% V_2O_5 is required on this alumina to reach a monolayer coverage (ca. 13 V atoms/nm^2). For most oxides, surface monolayer

coverage is 5–10 times higher than for silica [18,19]. As the loading increases, the interaction among the supported metal oxide species (M) increases, thus resulting in surface polymeric species, characterized by the formation of M–O–M bonds. Silica support presents such a weak interaction with the supported species, that only surface isolated or crystalline supported oxide species are observed. At the loading at which interactions among the surface isolated species appear the silica alone is unable to stabilize surface polymeric species and they aggregate into tridimensional crystals.

The importance of compounds resulting from the interaction of supported oxides with the support, like silicomolybdic acid on silica-supported molybdenum oxide catalysts can be excluded for ethane oxidation. Those species are not stable above ca. 570 K, breaking into surface molybdenum oxide species, as reported by several authors using different techniques [11,12,20,21] and no relevance is, thus, expected from silicomolybdic acid species for ethane oxidation, since the reaction is run well above 570 K. By contrast, the presence of additives affects the supported oxide. Alkaline additives and impurities (Ca, Na, K, etc.) tend to coordinate to acidic supported oxides (V, Mo, W, etc.) by altering the M–O bonds [22–25]. Acidic additives affect the structure of the supported species since the support sites must be shared with a second component, resulting in an effective increase in surface coverage [26,27]. The interaction with P, for supported vanadium oxide species may result in $VOPO_4$ if V is added prior to P; otherwise P coordinates strongly on the support. However, if silica is the support, its weak interaction with any supported species will allow the formation of $VOPO_4$ and of alkali vanadates irrespective of the preparation procedure [23,28–31], thus removing surface oxide species [17,25,29–32].

1.2. Activation of the hydrocarbon and selectivity

The activation of paraffins is harder than that of other hydrocarbons due to the high stability of the former. Therefore, the products formed may be readily oxidized under the conditions required to activate paraffins, thus limiting selectivity [33,34]. The high stability of alkanes is due to their electronic structure. The tetrahedral arrangement of C–H bonds protects the carbon atoms. The C–H bonds are more exposed than the C–C bonds of hydrocarbons and their cleavage should be the first step in the transformation of most hydrocarbons. The stronger the C–H bond is the stronger the activation must be, and the dependence of the optimal reaction temperature for selective oxidation on the binding energy of the C–H bond follows quite a linear trend for the lower alkanes [35]. The C–H energy bond is highest for primary carbons (Table 1), C–H bonds on secondary and tertiary carbons are more reactive and C_{3+} hydrocarbons are activated through these sites. However, all the carbons in ethane are primary, which makes it much less reactive than its larger homologues. The high dissociation energy of the C–H bond of ethane vs. that of other bonds in other molecules will affect the maximum selectivity attainable. By an extensive evaluation of activity data reported for several oxidation processes, Batiot and Hodnett have observed a correlation of the selectivity with the differences between the dissociation enthalpy of the weakest C–H bond (D^0H_{C-H}) in the reactant hydrocarbon and that of the weakest C–C or C–H bond of the product. Very high selectivity is observed if the difference is less than 30 kJ/mol, while it is minimal above 70 kJ/mol. A linear trend is observed for intermediate values, i.e., as the stability of the product vs. that of the reactant decreases [36]. Table 2 shows the dissociation enthalpy of the weakest C–H and C–C bonds in the products ethylene and acetaldehyde, together their difference with the weakest C–H bond of ethane (D^0H_{C-H}=420 kJ/mol). According to the data reviewed by Batiot and Hodnett, the conversion of ethane to ethylene is expected to be highly selective, with yields close to 50% (and some reports close to 60%). Burch [37] has also highlighted the lower reactivity of ethylene as compared to ethane for catalytic conversion. Conversely, the selectivity for

Table 1
Dissociation energy of C–H bond and charge on H of some light hydrocarbons

Hydrocarbon	Weakest C–H bond	C–H bond E_{disoc} (kJ/mol)	Atomic charge on H
Methane	Primary	440	+0.087
Ethane	Primary	420	+0.002
Propane	Secondary	401	−0.051
Isobutane	Tertiary	390	−0.088

Table 2
Dissociation enthalpy of the weakest C–H and C–C bond of ethene and acetaldehyde

Product	D^0H_{C-H} (KJ/mol)	D^0H_{C-c} (KJ/mol)	Lowest difference vs. Ethane D^0H_{C-H} (kJ/mol)	Expected selectivity
Ethylene	444	720	−24	High
Acetaldehyde	359	349	+70	Low

acetaldehyde is expected to be very low near 20% conversion ([36] and references therein). So, the relative reactivity of the reactant and the product determines the limiting selectivity under conventional reaction conditions. The formulation of the catalysts will affect their interaction with the reactant and the products. The activity of the hydrocarbons (both reactant and product), the activation of the oxidant, and the reactivity of lattice oxygen will determine how close the performance of catalyst is to optimal selectivity under conventional reaction conditions. Consequently, the maximum selectivity appears to be determined by the reaction, rather than by the catalyst.

The initial activation of the C–H bond of the hydrocarbon by the catalyst requires the existence of an affinity between the alkane and the surface of the catalyst. The acid–base interaction between the hydrocarbon molecule and the surface of the oxide promotes the approach of the former to the active site [33,38]. The surface acid/base features of an oxide depend on the charge and radius of the cation. The more oxidized the cation is, the more covalent the bond with the oxide ion, thus increasing the acidity of the oxide. Conversely, low valent cations result in a more electron-rich oxygen species, thus being more basic. The charges on the most reactive hydrogen atom of the hydrocarbons shown in Table 1 were calculated by Busca et al. [38]. Most of the alkanes have a negative charge on the most reactive hydrogen, which favors the interaction with electrophilic surfaces (acidic oxides). However, ethane and methane do not have a negative charge on the most reactive hydrogen, thus altering the nature of the interaction of these alkanes with the surface of the oxide as compared with larger hydrocarbons [38–44]. Methane clearly displays a positive charge on its H atoms and its activation is most effective on basic oxides. A certain correlation has been reported between the strength of basic sites on the oxide surface and the isotopic exchange reaction of methane with deuterium, Ga_2O_3 being the most reactive of the series of oxides tested by several orders of magnitude, and the ZnO being the second most reactive [45]. However, the rate of conversion of methane does not completely correlate with H–D exchange [46]. Ethane has a moderately positive charge in its H atoms, and probably, some stronger affinity may be expected with basic oxides than with acid ones, but no conclusive trend has been reported in this line. Larger hydrocarbons have a negative charge and should show stronger interaction with acidic catalysts [38–44].

The affinity between the hydrocarbon and the surface promotes the activation of the molecules. Selectivity is also determined by the hydrocarbon–catalyst interaction, the reactivity of the catalyst, and the stability of surface hydrocarbon species. A strong acid–base interaction with the support may also promote further degradation of partial oxidation products. Thus, higher hydrocarbons require basic sites to promote selectivity to olefins [33] such as for butane [22,47]. The appropriate use of alkaline additives increases selectivity at a given conversion. Concepción et al. [39] have shown that the selectivity to olefins in a series of catalysts depends on their basic character and on the specific hydrocarbon. *N*-butane increases its selectivity in the order MgVAPO-5<VO_x/Al_2O_3<VAPO-5<VO_x/MgO+Al_2O_3<VO_x/MgO; corresponding to a decrease in relative acidity, as determined by pyridine adsorption. This trend is reversed for ethane, while propane shows no specific trend at all [44]. In a different series (alkali-doped V_2O_5/TiO_2), the conversion in propane dehydrogenation decreases, but the yield to propene increases, due to a decrease in the heat of adsorption of propane [48]. The importance of the strength of acid sites has been reported since moderately acid sites promote the selective ODH of ethane, whereas strong acid sites promote non-selective CO_x species [18,49–51]. The performance of the catalyst is also affected by the acid–base characteristics of the hydrocarbon vs. that of the catalyst. The reactivity of the catalyst is also of great relevance, because it determines how fast the surface intermedi-

ates react. For instance, very high oxygen mobility is present in total oxidation catalysts, such as some perovskites [52,53]. By contrast, non-reducible oxides are much less reactive and require high reaction temperatures. These high reaction temperatures result in a significant contribution of the gas-phase radical reaction [37,54] and this is reported to promote ODH products during ethane oxidation [33,43].

1.3. Activation of the oxidant and selectivity

The oxidation of ethane involves activation of the organic molecule and of the oxidant. Activation of the oxidant depends on its nature. The activation of molecular oxygen requires the presence of a reducible oxide. For non-reducible oxides, the presence of dopants provides reducible sites for their activation [52]. In addition, the non-reducible catalysts operate at higher temperatures, which promotes the gas-phase activation of O_2 and C_2H_6 [37,54,55]. Molecular oxygen activation on reducible oxides has been estimated from the exchange of $^{18}O_2/^{16}O_2$ isotopes [45], which indicates the relative activation of oxygen on the surface of the oxides. This information offers a useful criterion for designing new catalysts [45]. The amount of defects in oxides, which is affected by the preparation method, strongly affects isotopic oxygen exchange [52,56–58] and this affects reactivity [56]. Since the present focus is on supported oxides, the properties of surface oxygen species are less sensitive to preparation procedures and the oxygen exchange properties are essentially affected by the surface coverage and surface–oxide interaction determine their properties. Chang et al. [59] have correlated the single-step double exchange between gas-phase $^{18}O_2$ and lattice (^{16}O) to form $^{16}O_2$ with the activity for oxidative dehydrogenation of ethane to ethylene on zeolite-exchanged and supported transition metal oxides. Both of them follow the trend: Co–H–ZSM-5 >Cu–Na–ZSM-5>V–ZSM-5>Nb–ZSM-5>Na–ZSM-5 H–ZSM-5Cu–ZSM-5. The formation of surface diatomic oxygen species can be observed by in situ Raman spectroscopy at moderate reaction temperature, but the band assignment is not conclusive [60]. In any case, these bands are not present at reaction conditions, thus suggesting that monoatomic surface oxygen species along with lattice oxygen may be involved in the conversion of ethane [60].

The relative ease in the removal of lattice oxygen is frequently characterized by the ease of catalyst reduction with hydrogen or hydrocarbon. Some reports show that the most selective catalysts are less reducible although sometimes this trend is reversed. However, catalyst reducibility is often determined by bulk reduction, which may differ from that of the surface sites. Since catalysis is a surface phenomenon, the data on catalytic performance should be correlated with the parameters of surface reduction rather than with those of bulk reduction. An interesting work by Valenzuela et al. [61] pointed out the relevance of surface reduction for ethane ODH. The activity corresponds to the surface reducibility determined by in situ XPS measurements, but not with bulk reducibility, determined by TPR. This observation is of key importance in understanding the performance of bulk oxide catalysts, but should also be considered for supported metal oxide catalysts above monolayer coverage. In addition to the relevance of surface vs. bulk reducibility, it should also be noted that under reaction conditions, the hydrocarbon and not molecular hydrogen is the reducing agent. The relevance of bulk reduction vs. surface reduction and the nature of the reducing molecule must account for some disagreements found when connecting the activity and reducibility of the catalysts. The selectivity and reducibility do not appear to show a clear trend. Even when a direct correlation if often observed between reducibility of supported vanadium oxide species and their activity, the oxidation state of the vanadium sites under reaction conditions does not correspond with the reducibility as observed by in situ Raman and Vis–UV spectroscopy under ethane oxidation conditions [14]. The average oxidation state of the vanadium site under reaction conditions, reflects the balance in the catalytic cycle of oxidation and reduction of the sites, and this will significantly affect the interaction with the hydrocarbon since the redox and acid–base properties are affected by the oxidation state. Since the oxidation state under oxidation conditions does not correlate with the reducibility, it must account for the lack of relation found between reducibility and selectivity. In situ studies are required to fully understand the factors affecting the selectivity.

The use of N_2O instead of molecular oxygen has proved to be more selective in the formation of C_2-oxygenates [31,62–66]. This appears to be due to the

strong activity of O^- species with alkanes at lower temperatures than under molecular oxygen. Ward et al. [63] observed the genesis of O^- species from N_2O but not from molecular oxygen upon interaction with the catalyst surface according to EPR spectroscopy. They detected no radical alkyl species, which suggests that radical species must readily transform into diamagnetic species [63]. Modeling by Sinev et al. [67] of the ethane-to-ethylene reaction requires activation of the alkane by cleavage of a C–H bond by surface-oxygen active species and a fast capture of ethyl radicals by surface oxygen active sites; this would account for the observations by Ward et al. [63]. The activation of N_2O seems to be related to the capacity of the oxide to undergo electron transfer to stabilize oxygen ions [52]. The reaction of O^- generated species with alkanes has been observed by EPR [68]. The interaction of N_2O with the catalyst is different to O_2 since nitrous oxide does not fully reoxidize the catalyst under reaction conditions [31,69] and the activation energy is different when oxygen or nitrous oxide are used as oxidants for ODH of ethane [70]. Additionally, the reaction in the presence of N_2O appears to be less affected by the modification of the redox properties of the catalyst. Supported-oxides, undoped and doped with K, afford similar conversions of ethane under N_2O. Conversely, the activity decreases remarkably upon the addition of K if the reaction in run under O_2 [22,31,71], as expected from the relevance of reducible sites for the activation of molecular oxygen. Comparison of both oxidants is hard since N_2O requires lower operation temperatures than O_2. At low temperature, N_2O has been reported to be more active than molecular oxygen for the oxidation of methane to formaldehyde on vanadium oxide catalysts, whereas the situation is reversed at higher temperatures [72,73].

Reductive activation of the oxidant (oxygen or nitrous oxide) with hydrogen significantly increases the conversion of ethane and decreases the reaction temperature to the 573–773 K range. While the dehydrogenation predominates when oxygen is used as oxidant, the use of nitrous oxide, or the addition of hydrogen with any of the oxidants shift the product distribution to the oxygenates ethanol, ethanal and formaldehyde [66].

The presence of surface electrophilic oxygen species is associated with the non-selective oxidation of hydrocarbons, whereas nucleophilic oxygen species promote selective oxidation [52,53,74]. However, combustion of ethane has been observed in the absence of gas-phase oxygen, the oxide being the only source of oxygen [53] since the mobility of oxygen in the oxide is an additional factor determining selectivity [52]. Factors governing the activation and stability of the hydrocarbon and intermediates also affect the activity and selectivity of the process.

1.4. Experimental conditions

The temperature at which ethane ODH is run under molecular oxygen may promote gas-phase conversion of ethane, since this becomes significant above 923 K [37,44,55,57,75–81]. The participation of gas-phase reaction should be prevented to avoid additional sources of reactivity. This would confuse the evaluation of catalytic performance. The relevance of the gas-phase conversion is directly related to the amount of void volume present in the reactor [55,78]. As the surface-to-volume ratio of the reactor increases, the relevance of gas-phase conversion of ethane is minimized since radicals are terminated by collision with the walls of the reactor or by adding inert packing to the reactor that will scavenge the radicals. On the other hand, the interaction with the walls of the reactor may also provide further activation of ethane if the reactor contains trace amounts of the catalyst. Consequently, the contaminated walls themselves would act as a catalyst, thus altering the catalytic evaluation [57]. The presence of water in the reaction feed, decreases the conversion and increases the selectivity to oxygen containing species [82].

The reaction under N_2O occurs at lower temperatures than under O_2, which would prevent the participation of gas-phase reactivity. The presence of water, however, has a dramatic effect on the activity. The presence of 25 Torr of water on silica-supported molybdena catalysts under N_2O decreases conversion by 80% at 550 K while lower amounts of water have no appreciable effect [63]. The presence of water promotes the ODH of ethane in the gas-phase at 860 K under O_2. At moderate reaction temperatures, partial solvating of surface vanadium oxide species, that would affect the catalytic properties, has been observed by in situ Raman spectroscopy [83]. However, such hydration is not observed for silica-sup-

ported catalysts, due to the hydrophobic character of silica, and no modification in the structure of surface molybdenum oxide species is expected. However, the presence of large amounts of water must affect somehow the activation of N_2O into O^- species [63], since O^- species are not observed by EPR on water-exposed silica-supported molybdenum oxide catalysts under N_2O at 363 K [84]. However, 363 K is a rather low temperature, and some surface hydration is expected [83]. Hence, this experiment may not reflect the reaction conditions. The addition of water to the feed decreases the formation of ethylene and increases that of CO and acetaldehyde, but has no effect on CO_2 formation.

2. Ethane ODH and partial oxidation to oxygenates

2.1. Vanadium oxide-based catalysts

V-containing catalysts have been extensively used in a large number of catalytic processes involving selective oxidation reactions (such as the conversion of butane to maleic anhydride, oxidation of *o*-xylene, 1,3-butadiene, methanol, CO, ammoxidation of hydrocarbons, selective catalytic reduction of NO, and the partial oxidation of methane) [25,34,85,86]. The applicability of vanadium-based catalysts for ethane conversion are evident [87–90]. This section will evaluate the relevance of several parameters on the performance of supported vanadium oxide species.

2.1.1. On the active oxygen site

Like other reactions, the terminal metal–oxygen double bond has been proposed to be the active site for selective oxidation of hydrocarbons [91,92], however, INDO calculations by Haber et al. [93] suggest that the interaction of a hydrocarbon molecule is most favorable with a bridging oxygen than with a terminal one for vanadium oxide clusters. When the relevance of the terminal V=O bond for ethane oxidation on supported vanadium oxide catalysts at monolayer coverage on several supports is evaluated by in situ Raman spectroscopy, it turns out that the V=O bond does not correlate with the changes of activity of the catalysts, which are of one order of magnitude [18]. Similar results have been reported by Wachs and coworkers for butane oxidation [15] and methanol oxidation [94]. This would indicate that the terminal V=O bond does not appear to be involved in the catalytic oxidation of ethane. Furthermore, several experimental evidences support the relevance of bridging oxygens for selective oxidation of hydrocarbons. Initially, studies on molybdenum oxide suggests that the oxygen involved in catalytic selective oxidation is the bridging one [95]. Combined Raman and isotopic labeling on β-$VOPO_4$ suggests that the V–O–P oxygen is involved in the selective dehydrogenation of C_4 hydrocarbons, while the contribution from the terminal V=O bond to this selective process appears to be very reduced [96]. The same methodology allowed Glaeser et al. [97] to show that the bridging Bi–O–Mo in bismuth molybdate participates in the selective oxidation of hydrocarbons. The contribution by Chaar et al. [98] on magnesia–supported vanadia with high selectivity for butane dehydrogenation evidence the absence of terminal V=O bonds by IR spectroscopy. It therefore appears that the terminal oxygen is not critical for the selective oxidation of hydrocarbons. In fact, an in situ isotopic Raman study with $^{18}O_2$ by Wachs and coworkers [15] revealed that the terminal V=^{18}O bond is stable for nearly 20 times the characteristic reaction time. More recently, the same group has reported that, in different environments, vanadium has the same activity irrespective of the presence of the terminal V=O bond [99]. A very recent contribution by Dang et al. [100] on the dehydrogenation of ethane on $BaCO_3$–supported vanadia has demonstrated the formation of $Ba_3(VO_4)_2$, which is highly selective (76% selectivity of ethylene at 34% conversion at 923 K) and has no terminal V=O bonds. Thus, it is the bridging bond that must be invoked to account for this catalytic performance. All these results rule out the terminal V=O bond as the critical active site of supported vanadium oxide catalysts for the oxidation of ethane.

2.1.2. Support effect (V–O-support bond)

The oxygen species bridging surface vanadium oxide species to the support may play a significant role in catalyst activity. A change in the support changes the V–O–S bond and the catalytic performance for ethane oxidation is affected by one order of magnitude in the sequence TiO_2>ZrO_2≫Al_2O_3>Nb_2O_5>CeO_2–SiO_2 [18]. The change in support alters

the TOF number by four orders of magnitude for methanol oxidation and two orders of magnitude for butane oxidation [15,94]. These results suggest that the bridging V–O–S bond would be directly involved in the reactivity of supported vanadium oxide species. The evaluation of vanadium sites in different environments by Wang et al. [99] underlines the relevance of the V–O–S bond for activity vs. the terminal V=O bond. The nature of the V–O–S bond appears to be critical for the oxidation of ethane. The activity order is close to the reducibility of surface vanadium oxide species on these supports, which correlates with the Sanderson electronegativity of the cation of the oxide support [14,101]. However, this trend follows as CeO_2>ZrO_2–TiO_2>Nb_2O_5>Al_2O_3>SiO_2. Ceria and niobia react with the supported vanadia, forming new compounds that remove surface vanadia species [14] thus decreasing their activity. The presence of an acidic support (alumina) also increases activity but to a lesser extent than a reducible support. The higher reducibility results in a higher TOF number, but oxidation state under reaction conditions does not correspond with the reducibility, as observed by in situ Raman and Vis–UV spectroscopy [14]. The stability of the supported vanadium oxide catalyst is an important factor. Reducibility of V on SnO and CeO_2 is high but the activity is low. When tin oxide is used as a support for vanadium oxide it promotes its integration into the rutile lattice of SnO as V^{4+} [102]. A similar phenomenon takes place for titania–supported vanadium oxide, which decreases its activity due to integration of V^{4+} sites into the rutile phase of titania, along with the utilization of anatase phase [18,103–105]. It should be noted that the lower activity of rutile–supported vanadia is due to the integration of vanadium species into rutile lattice, as the activity of surface vanadium oxide species is not affected by the specific oxide support phase [106]. It has been shown that the structure (according to Raman spectroscopy and ^{51}V-NMR) and reactivity of surface vanadia species for methanol oxidation is not affected for a series of titania–supported vanadia on a series of titania supports possessing different phases (anatase, rutile, brookite and B) [106]. As commented above the low TOF numbers for V_2O_5/Nb_2O_5 and V_2O_5/CeO_2 are due to a solid state reaction with the support [14].

The effect of the acidity of the support in ethane oxidation with molecular oxygen on supported vanadium oxide catalysts has been explored by Le Bars et al. [51] and Wan and coworkers [50]. Activity decreases in the order V^{5+}–ZSM-5>V^{5+}–APO-5 >$V^{5+}/AlPO_4$>V^{5+}/silicalite>V^{5+}/silica [50]. This trend corresponds to the number of acidic sites. All the catalysts show comparable selectivity of ethylene and CO. The higher activity of ZSM-5–supported vanadium oxide catalyst is also related to the large amount of CO_2 that may arise from over oxidation of partial oxidation products inside the microporous structure. The stronger acidity observed for P-containing catalysts appears to be due to the P–O–V bond, since XPS technique reveals a strong electron withdrawing effect on vanadium sites [50]. The higher activity of V–APO-4 catalyst is also related to the higher ease of reoxidation [50].

Both, acid–base and redox properties affect the conversion of ethane. López-Nieto and coworkers [39,107] have reported the equilibrium required between reducibility and the acid–base character of the sites. These authors studied the activity of highly dispersed surface vanadium oxide species on alumina, magnesia, mixed magnesia–alumina, and vanadium oxide-containing microporous material. As in other reports [18,30,40,61,71,108], the activity under O_2 runs parallel to the reducibility of the catalysts, which decreases thus: V_2O_5/Al_2O_3>VAPO-5>MgAVPO-5 V_2O_5/MgO>$V_2O_5/MgO+Al_2O_3$. However, the selectivity of olefins depends on the acidity of the catalysts, which increases as V_2O_5/MgO<$V_2O_5/MgO+Al_2O_3$<VAPO-5<V_2O_5/Al_2O_3<MgVAPO-5, as determined by pyridine adsorption [39,107]. Michalakos et al. [40] have observed the same trend for supported vanadia catalysts with Mg or P. It has also been reported that for vanadium oxide and magnesium oxide supported on APO-5 catalysts [109] the acid–base and redox function must be near the V sites. Modification of vanadium sites reducibility with Co on CoVAPO-5 further increases activity while ODH selectivity remains reasonably high [107]. The beneficial effect of Co is also an expected result in view of the temperature-programmed isotopic exchange studies by Chang et al. [49] on several ZSM-5-based catalysts. This confirms that also reducibility and acid–base properties determine the performance for ODH. The former is related to the activation of the hydrocarbon, but the ability to activate oxygen (isotopic exchange) provides additional reactivity.

2.1.3. Surface vanadium oxide coverage effect (V–O–V bonds)

Surface coverage alters the population ratio of (V–O–V)/(V–O-support) bonds. This trend is not observed on silica-supported vanadia, where isolated surface vanadium oxide species are dominant up to monolayer coverage. V–O–V bonds appear to be involved in ethane oxidation, as observed by in situ Raman spectroscopy [14]. The same trend has been observed under butane oxidation [16]. Surface coverage has a much lower effect than the nature of the support oxide. However, the environment of surface vanadium oxide species must affect the activity of the oxide catalysts, since neighboring surface vanadium oxide species promote the reducibility, thus increasing the activity. At very low surface coverage on alumina, the addition of vanadium decreases acidity, as the alumina sites are covered [110]. Above monolayer coverage, no further increase of acid sites is observed. Activity increases with V loading on alumina–supported vanadia catalysts but the TOF number remains essentially constant [14,18,44,111]. Selectivity is affected by alumina coverage: at low vanadium coverage, carbon dioxide is the main oxidation product, mainly due to the alumina sites. At higher V loading the alumina sites are titrated by surface vanadium oxide species and the selectivity increases reaching a yield of 21% for the 3.3% V_2O_5/Al_2O_3 catalyst. At very high V loading tridimensional bulk-like vanadia species are dominant. Their catalytic performance yields ODH products and non-selective CO_x species. The surface coverage of vanadium on alumina modifies the acidic and basic features of the catalyst [110,111]. The TOF number on silica–supported vanadium is constant up to ca. 5% V_2O_5/SiO_2 and decreases at higher loading due to the formation of vanadia crystals [14,111]. A similar trend has been observed for methane conversion to oxygenates [112] with vanadium loading on silica. In general, selectivity is affected by the coordination of vanadium oxide sites since the presence of V–O–V bonds with increasing coverage of vanadium decreases the selectivity to ethylene [18,39], it may be due to a larger number of active sites that may attack the hydrocarbon molecule. In fact, the site isolation proves to improve selectivity [33,34]. In this line, it is interesting to note that the best selectivities are reached on silica–supported oxides. It should be noted that no surface polymeric species are observed in silica–supported vanadia under dehydrated conditions, and only surface isolated vanadium oxide species are present up to monolayer coverage as measured by Raman and ^{51}V-NMR spectroscopy [7,8] and by ^{51}V-NMR and TPR measurements [113]. This is not the case on other supports like alumina. Oyama and Somorjai [114] have observed lower selectivity at low surface vanadium loading on silica. At high surface coverage, ethylene is the main oxidation product whereas at low surface coverage CO_2 is the main oxidation product. However, no characterization of these catalysts has been provided to explain why these vanadia silica catalysts show trends different from those of other silica–supported catalyst series. The formation of selective oxygen-containing products (mainly acetaldehyde) is only observed at high vanadia surface coverage on silica by these authors [114].

2.2. Molybdenum oxide-based catalysts

Silica–supported molybdenum oxide was tested for ethane oxidation with nitrous oxide by Ward et al. [63]. EPR and XPS experiments showed that partially reduced Mo^{5+} species are directly related to the active site. They proposed that c.u.s. Mo^{5+} species would be the active site and that nitrous oxide would be activated to O^- species, which readily react with ethane to yield ethylene at reaction temperatures below 573 K. The absence of paramagnetic signals for surface ethyl radical rules out the presence of long-lived radical intermediates [63], in agreement with the foreseen rapid reaction of surface oxygen species [67]. If molecular oxygen is used instead of nitrous oxide, activity is very low and a certain activity is only seen at higher temperatures. By contrast, molybdenum oxide species are visibly oxidized, which is not the case under N_2O. A completely oxidized MoO_3/SiO_2 catalyst is not active for the oxidation of ethane [115]. In fact, the activity of MoO_3/SiO_2 in O_2 is comparable to that of pure silica [116]; thus, MoO_3/SiO_2 is not active for ethane oxidation in molecular oxygen at low temperatures. The presence of water vapor is essential for high selectivity to acetaldehyde. Surface molybdenum coverage on silica is of crucial importance for the activity and selectivity of the catalyst. No systematic study has been carried out yet on the effect of the support for supported molybdena, but the Mo–O-

support bond has been proposed as the critical bond for methanol oxidation [6], it is expected that it will also be the critical site for ethane oxidation, as in the case of supported vanadium oxide catalysts. It appears that surface molybdenum oxide species interacting with silica are active for acetaldehyde formation. At higher loading a tridimensional molybdenum oxide structure is expected to dominate. At this molybdena loading the selectivity is lower [39,42]. As for other oxides, the oxide used as a support affects the performance of the supported molybdenum oxide species, but to a lesser extent than in the case of vanadium oxide [101]. The very different trends with molecular oxygen or nitrous oxide as oxidants point to the existence of different mechanisms for each oxidant. The reaction is of first order with respect to N_2O but zero order with respect to O_2. As reported by several authors, N_2O is more active than O_2 at low temperature, whereas at high reaction temperature this reactivity order is reversed [30,62,70,71].

2.3. Alkaline and metal additives

Alkali doping has afforded positive effects in many catalytic processes, like the synthesis in ammonia, the oxidation of SO_2 to SO_3, or the dehydrogenation of ethylbenzne to styrene, among others [117]. As regards supported metal oxides, alkaline additives tend to coordinate to acidic surface species (V, Mo, etc.), affecting the V–O bonds [22–25,118]. The presence of alkaline additives has a beneficial effect for the dehydrogenation of larger hydrocarbons due to a modification on the acid–base interaction of the hydrocarbon with the catalyst [37], but this trend reverses for ethane [44]. If silica is the support, compounds form readily with alkaline additives, due to the very weak interaction of silica with the supported species [17,25,29–32]. The new compounds arising from this interaction show different performance due to new structural, acid–base and redox properties. Thus, Li, Na, K, Rb and Cs on silica–supported vanadium oxide form the corresponding vanadates, as reported by Erdöhelyi and Solymosi [31]. Except for KVO_3/SiO_2, all the catalysts undergo deactivation slowly during the oxidation of ethane with N_2O. The deactivated catalyst can be regenerated, except $NaVO_3/SiO_2$, by oxidation at 773 K. $NaVO_3$ is not stable above 720 K and decomposes. The rest of the alkali-vanadate catalysts have higher stability than silica–supported vanadia catalysts and the formation of acetaldehyde and CO_2 is considerably higher, while that of ethylene and CO decreases for the oxidation of ethane with oxygen [22]. The addition of K decreases the activity of alumina–supported vanadium oxide catalysts under O_2 (Table 3) [22], contrary to the effects of alkaline additives observed by Solymosi [30,31] when N_2O was used as oxidant.

The marked difference in performance of V_2O_5/Al_2O_3 and V_2O_5/SiO_2 catalysts upon addition of K must arise from the kind of oxidant used since it has been reported that nitrous oxide activation only requires single isolated sites [52], whereas the activation of molecular oxygen may have further requirements. The presence of alkaline additives of silica–supported molybdenum oxide catalysts has a similar effect to that observed for vanadia-based catalysts [119]. Activity remains comparable when nitrous oxide is the oxidant, while it decreases remarkably when the oxidant is molecular oxygen. The presence of alkaline additives affects the redox properties of supported oxides (Mo or V) [17,22,30,71,119]. In the presence of oxygen, the reaction appears to involve redox cycles in the oxide catalysts. The addition of alkaline dopants decreases the extent of the redox properties of the supported oxide, thus decreasing the performance. The reaction in the presence of nitrous oxide does not appear to involve a redox cycle in the oxide and the interaction of N_2O oxidant with the catalysts does not appear to be decreased by alkaline additives. However, for both oxidants the selectivity to CO_x products is higher than in alkali-free supported oxides. The larger production of CO_x products may be associated with the higher basicity of the catalyst, which should alter the interaction between the hydrocarbon and the catalyst surface [39].

Erdöhelyi and Solymosi [29,119,120] evaluated the performance of alkali-molybdates supported on silica. All the alkali molybdates showed similar reducibility, which was much lower than that of silica–supported bulk molybdena. The number of basic sites increases from Li to Cs molybdate. Silica–supported molybdena deactivates during the oxidation of ethane with nitrous oxide. The catalysts are reactivated by reoxidation. Cs-, Rb-, and K-molybdates are active under the same conditions, but Na- and Li-molybdates show no

Table 3
Performance of supported vanadium oxide catalysts with different oxidants

Oxidant	Catalyst	Temperature (K)	Conversion (%) C_2H_6	Selectivity (%)					References
				C_2H_4	CO	CO_2	CH_3CHO	C_2H_5OH	
N_2O	KVO_3/SiO_2 (1.2 V at./nm^2)	823	9.2	38.9	15.7	30.1	13.8	1.5	[19]
	2% V_2O_5/SiO_2 (1.2 V at./nm^2)	823	6.9	50.6	35.7	8.9	4.8	–	[17]
O_2	5% V_2O_5/SiO_2 (1.4 V at./nm^2)	803	5.6	62.0	18.1	5.7	11.2	0	[18]
	2% V_2O_5/SiO_2 (1.2 V at./nm^2)	811	30.0	22.0	–	–	3.0	0	[71]
	V_2O_5/Al_2O_3	803	24.8	53.7	40.7	5.5	0	0	[22]
	$K+V_2O_5/Al_2O_3$	803	6.2	39.1	34.7	26.0	0	0	[22]

Reaction conditions: [30,71], *ca*. 0.8 g catalyst, 20% C_2H_6+40% oxidant in He; [18], 20 mg, 30 ml/min, C_2H_6/O_2/He=1/2/8 mole ratio; [22], 500 mg, 200 ml/min, C_2H_6:O_2:He=4:8:76.

improvement. The yield to acetaldehyde increases with cation size, but decrease with time, like the yield of CO_2. However, ethylene remains constant. The deactivation is due to an increasing reduction of the catalyst, which is regenerated upon reoxidation [29]. Again, water vapor favors acetaldehyde formation, especially for Rb_2MoO_4 (selectivity increases from 20% to 33%). The data presented by Erdöhelyi and Solymosi suggest the relevance of acid sites for ethane oxidative dehydrogenation and of basic sites for acetaldehyde formation. Comparison with $ZnMoO_4$, $MgMoO_4$ and $MnMoO_4$ further evidences these trends [119].

The addition of acidic niobia has no effect on the structure of supported vanadium oxide species [25,121], it simply increases the surface density of vanadia sites [25]. This increases the amount of surface polymeric species, except for silica, where no surface polymeric species are observed [25]. The addition of niobia to vanadia titania catalysts modifies the redox properties and increases the acidic properties of the V_2O_5/TiO_2 catalyst; this increases the selectivity to ethylene [121]. This would suggest a beneficial effect of acidic sites for the ethylene, but more results are required to fully substantiate this statement for the oxidation of ethane.

2.4. Phosphorus-containing catalysts

2.4.1. Catalysts containing V and P

Merzouki et al. [122] evaluated the performance of VPO catalysts. If the P/V atomic ratio is 1.15/1 activity is very low and acetic acid is the only product formed at low temperature. Increasing the oxygen-to-ethane ratio in the feed increases the acetic acid-to-ethylene selectivity ratio but has no effect on carbon dioxide formation. Doping the VPO catalysts with Te (Te/V=10%) decreases the selectivity of the catalyst. Conversely, Pd-doped VPO (Pd/V=0.15–1%) increases activity with Pd loading; acetic acid is already observed at 473 K and acetic anhydride at 573 K. However, the most remarkable feature of Pd-doped VPO catalysts is that, as conversion increases, ethylene becomes the main oxidation product with selectivity above 90% at ca. 12% conversion. The addition of Te yields a new structure of $Te_2V_2O_9$ along with the $(VO)_2P_2O_7$ phase, whereas Pd-doped VPO catalysts show no new compounds with Pd. However, only the very first layers are directly involved in the reaction. The presence of Te promotes the V^{5+} oxidation state and Pd results in 95% of V^{4+}. This may account for the different performances observed after doping with Pd or Te (Fig. 1). It has been proposed that the high affinity of metallic Pd for H_2 accounts for the high selectivity of ethylene.

Tessier et al. observed that among bulk VPO catalysts ($\alpha VOPO_4$, $(VO)_2P_2O_7$ and $VO(PO_3)_2$) only $VO(PO_3)_2$ appears to oxidize ethane to acetic acid. Acetic acid selectivity is 100% up to 573 K, but activity is very low (<0.1%) and decreases rapidly over time [123]. Supporting this VPO catalyst on titania support prevents deactivation for atleast five days on stream. Conversion is higher and acetic acid is observed at 473 K, but its selectivity decreases with conversion (temperature). High pressure (10 bar) increases the production of acetic acid. The effect

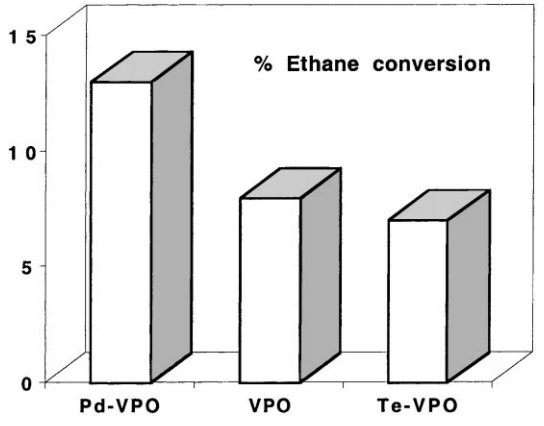

Fig. 1. Conversion of ethane on pure VPO catalysts, and when doped with Pd or Te [122]. Reaction conditions: 673 K, τ=3.8 s, $O_2/C_2H_6/N_2$=2.5/5/92.5.

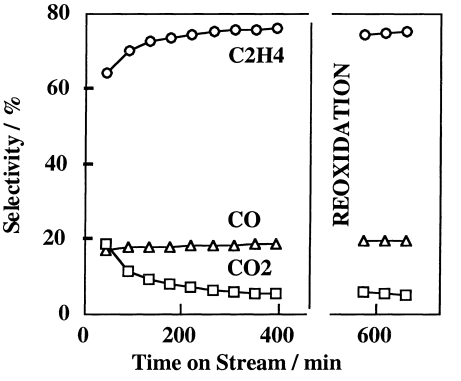

Fig. 2. Selectivity of ethylene (circles), of carbon monoxide (triangles) and of carbon dioxide (squares) of a V_2O_5/alpha-Ti phosphate during time on stream [125]. Reaction conditions: 723–863 K, total flow: 30 ml/min, O_2/C_2H_6/He=6/1/8 mole ratio, 60 mg of catalyst.

of high pressure, shifting the reaction towards oxygenate formation, has been observed in the homogeneous conversion of ethane by Gesser et al. [124]. As in other catalysts, the presence of water vapor also promotes the formation of acetic acid [71,78,82,122].

Santamaría-González et al. [125] have just reported the oxidative dehydrogenation of ethane on vanadium oxide supported on layered α-titanium phosphate (α-TiP). This is a selective catalyst for ethylene production, with negligible production of CO_2. The participation of the gas-phase reaction was prevented and the catalyst is stable on stream for atleast 24 h. A strong interaction between V and P sites is seen with XPS. In situ Raman spectra provide evidence about the formation of a new surface compound, which is not formed under calcination of the precursor of the catalyst. The reaction conditions, promote the rearrangement of the surface vanadium oxide and surface phosphate species forming the $VOPO_4$ phases [125]. The formation of this new phase must be associated with the transient period during which activity increases, and the selectivity of ethylene increases at the expense of the non-selective CO_2 (Fig. 2). The bridging V–O–P sites formed under reaction conditions must provide the new selective site, which further supports the results reported by Lashier at al. [96] on the relevance of the V–O–P bonds for the selective oxidation of hydrocarbons. The vanadium oxide supported on layered Zr phosphate is less active, but selectivity is still high [126]. The relevance of P as additive has been observed for V-based catalysts on alkane oxidation reactions [16,34].

2.4.2. *Catalysts containing Mo and P*

As in the case of V, the presence of P results in a new catalytic performance for Mo-based catalysts. Thus, Hong and Moffat [62] evaluated the performance of 12-molybdophosphoric acid (HPMo) for ethane oxidation. The relevance of bulk heteropoly acids in catalysis is well-known [127]; similarly to oxides, the use of a support has several advantages: Moffat and coworkers had already reported the benefits of supporting heteropolyacids, since the activity for this reaction increases by a factor of 10 [128]. Non-polar molecules such as ethane are unable to penetrate into the large bulk structure of heteropolycompounds. However, this interaction can be facilitated by depositing the 12-molybdophosphoric acid onto a suitably high-area support. Loading of ca. 20 wt% allows highly exposed heteropolyacids (small aggregates), such as 12-molybdophosphoric acid to become accessible to ethane molecules, while high surface loading leads to large aggregate formation of HPMo on the silica, rendering a significant amount of the catalyst inaccessible to the ethane molecules [62]. Acetaldehyde and ethylene are the main oxidation products (ca. 44% and 41% selectivity, respectively) on silica–supported 12-molybdophosphoric acid. The catalysts show some deactivation during time on stream, but this is quite moderate at low reaction temperatures

(650 K). This could be due to decomposition of the heteropolyacid into the constituting oxides. The kinetic orders for ethane and nitrous oxide were 0.7 and 0.6, respectively. TCM was added to increase activity, but did not significantly alter the selectivity trends. Cavani et al. [2] found a similar trend during HCl pulses. The use of chlorine-based additives to promote activity is discussed below. The lower selectivity under molecular oxygen is again evidenced here, since it decreases to a third the selectivity of acetaldehyde and increases that of CO [2,128]. The selectivity trends suggest that ethylene and acetaldehyde are primary products. Pulse experiments support the notion that acetaldehyde is essentially associated with a catalytic process while ethylene participates from gas-phase reactions [41] and this may account for the shift in selectivity trends to ethylene from acetaldehyde as reaction temperature increases [62].

The relevance of different formulations of heteropolyoxometallates has been recently studied by Moffat et al. [41] and by Cavani et al. [2] in view of the possibility of tuning the acid–base and redox properties of these compounds. Since structural stability under reaction conditions may be limited, the addition of Sb (1 Sb atom per Keggin unit) stabilizes the structure of 12-molybdophosphoric acid by ca. 90 K, but catalytic activity decreases as Mo^{5+} is stabilized, thus limiting redox functionality [2,129]. The incorporation of Cr or Ce to the Keggin unit did compensate the redox properties if the loading values were below 0.5 atoms per Keggin unit. A higher amount of Ce further increases activity, but selectivity decreases markedly. Cr addition follows trends similar those to Ce. Partial replacement of Mo by W improves the performance by addition of up to one W atom per Keggin unit [2]. In addition, tungstophosphoric acid structure presents higher acidity than molybdophosphoric structures, as predicted from extended Hückel calculations [130] and determined experimentally [41]. The acid–base properties can also be tailored by the addition of P, which increases surface acidity, thus favoring ethylene formation. The addition of a second cation also influences morphological properties [41]. The combined use of Sb and K stabilizes the structure, while selectivity remains completely unaffected [2,129]. The heteropolymolybdates tested by Li and Ueda [131] show a 10% selectivity of acetic acid at 1% conversion.

2.4.3. Mo and V P-based catalysts

V–Mo phosphates, VPO and MoPO materials supported on titania–anatase were evaluated for the conversion of ethane to acetic acid by Roy et al. [132]. Pure bulk $(VO)_2P_2O_7$ and $(Mo)_2P_2O_7$ show very low activity (0.2% conversion) and do not produce acetic acid. The activity of VPO catalysts appears to be associated with the presence of extended defects [133]. The use of a support for VPO catalysts is expected to increase the exposure of the sites and to promote the formation of defects in the VPO structure, thus increasing its activity. The Mo–V phosphate catalyst supported on titania is active for acetic acid formation and presents low selectivity of ethylene. The best performance corresponds to a Mo–V phosphate on titania–anatase at low surface coverage. Raman spectroscopy shows that molybdenum and vanadium oxide species spread onto the support as surface dispersed oxide species, thus accounting for the coverage of the titania surface sites. The relevance of reaction conditions in the spreading of metal oxides has been observed with in situ Raman spectroscopy [134]. In this sense, it is interesting to note that above 1.6×10^{-2} (Mo+V)/Ti loading activity decreases (Table 4), possibly indicating that the surface dispersion of V and Mo species is no longer possible due to saturation of the titania sites. This points to the relevance of the titania support for the generation of active sites, and strongly suggests that active species are surface sites formed by decomposition of the phosphate compound. Several studies suggest that the active sites of VPO catalysts are associated with the formation of surface species formed under reaction and interacting with the VPO substrate [14,135].

2.5. Boron oxide based catalysts

The oxidation of ethane to acetaldehyde is essentially accomplished using nitrous oxide as an oxidant, but the need for a catalyst able to convert ethane into C_2 oxygenates in the presence of molecular oxygen is evident. The group of Otsuka evaluated the performance of the oxidation of ethane with molecular oxygen of the oxides of B, Mg, Al, Si, Ca, Ti, V, Cr, Mn, Fe, Co, Ni, Cu, Zn, Ga, Sr, Y, Zr, Nb, Mo, Cd, In, Sn, Sb, Te, Ba, La, Ce, W, Pb, and Bi. Only the oxides of B, Al and Si produced oxygenates. However, alumina and silica produced mainly CO_x. Supporting

Table 4
Ethane oxidation on V–Mo–P/TiO_2 catalysts [132]

(Mo+V) 100 Ti	Mo/V ratio	Conversion (%)		Selectivity (%)				Yield (%) CH_3COOH
		C_2H_6	O_2	C_2H_4	CH_3COOH	CO	CO_2	
1.5	10	0.7	5	6	48	28	18	0.34
1.5	4	1.5	12	6	34	34	26	0.51
1.5	1	3.2	29	8	21	44	27	0.67
0.8	4	0.6	2.5	1	32	31	36	0.19
1.6	4	1.5	12	6	34	34	36	0.51
3.2	4	1.1	8	11	36	34	19	0.40

Reaction conditions: Feed $C_2H_6/O_2/N_2/H_2O$=62/17/11/10 molar; GHSV=480 h^{-1}; T=548 K.

B on alumina, magnesia, lanthanum and P_2O_5 improved the catalytic performance of boria [116]. Boria on alumina and on zinc oxide were the most active catalysts. The yield of ethylene was near 14.5% for both catalysts, but the highest yield of acetaldehyde in the alumina-supported series (1.03%) is attained with by B_2O_3/Al_2O_3, whereas zinc–supported boria produce no detectable amounts of acetaldehyde. It is interesting to note that B_2O_3/P_2O_5 and B_2O_3/TiO_2 show very high selectivity to ethylene (89.7% and 98.0%, respectively). As boria loading on alumina increases, both conversion and selectivity increase since B covers non-selective alumina sites in a similar fashion to other alumina-supported oxides [14,44,110]. Microcalorimetric evaluation of the acidity of alumina and boria–alumina materials performed by Colorio et al. [76,136] reveal that strong acid sites of the alumina support were replaced by a large number of weak acid sites upon addition of boria. At the same time, the conversion of ethylene and the selectivity for acetaldehyde increases with boria content up to a boria loading of 30% on alumina, where tridimensional boria aggregates are evident and surface area decreases markedly. The presence of highly dispersed B oxide species interacting with alumina, evidenced by XPS, is associated with the formation of acetaldehyde whereas the crystalline boria is associated with the ODH reaction [116]. The most remarkable feature is that highly dispersed boron on alumina performs for the oxidation of ethane with molecular oxygen at a level comparable with that of silica–supported molybdena with nitrous oxide as oxidant. The data presented by the authors indicate that two kinds of sites are present on boria–alumina catalysts: those leading to the ODH reaction and those leading to the formation of C_2 oxygenates. CO_x and CH_4 appear to be formed from acetaldehyde, as suggested by yield trends vs. residence time. The dominant mechanism appears to be radical, since boria may not participate in redox cycles. It is proposed that ethane is activated through the abstraction of H by adsorbed electrophilic oxygen species; a second H-abstraction should form ethylene. Reaction of the ethyl radical with molecular oxygen forms ethylperoxy radical, which must be in equilibrium with ethyl radicals in the gas-phase. Reaction with ethyl radicals forms ethylhydroperoxy radicals which may decompose to ethylene or to acetaldehyde. This appears to be the faster route to ethylene. According to the calculations by Sinev et al. [67] on the oxidation of ethane on PbO/Al_2O_3 catalysts, the ethyl species formed from ethane react fast with surface O species and the O–containing surface intermediates can yield ODH products. The presence of oxygenate precursors of hydrocarbons has also been reported for methane formation by in situ IR and MS studies [137]. As observed by Otsuka et al. [116], the boria–alumina catalyst showed no deactivation, and it is interesting to note that the preparation method (impregnation and chemical vapor deposition of the boron oxide precursor on alumina) revealed no differences in the catalytic performance below monolayer coverage. However, no acetaldehyde formation was reported by these authors.

Otsuka et al. evaluated the use of BPO_4 catalysts for ethane oxidation. Acetaldehyde, formaldehyde, CO_x and ethylene were observed [133]. Pure BPO_4 is not active but treatments under reaction feed over 20 h at 823 K results in an active system [138] with a selectivity for acetaldehyde of 54.5%. Experimental evidence suggests that surface boron oxide species

interacting with a BPO_4 structure must be the active site for acetaldehyde formation. A similar phenomenon has been observed for boron on MFI zeolites under propane oxidation [139]. The formation of the aldehyde increases with B doping up to a critical loading value where crystalline boria is expected to develop and ethylene becomes the dominant product at the expense of acetaldehyde [138]. This is consistent with the performance previously observed for bulk boria on alumina. The nature of the boron species and its mechanism for the oxidation of ethane to acetaldehyde has been calculated using quantum chemical cluster calculations. Under reaction conditions, pure BPO_4 is expected to rearrange its surface, generating Lewis acid three-coordinated boron sites [138], while the four-coordinated B inside the BPO_4 structure is inactive because it is not accessible [140]. Ethane adsorbs dissociatively on the Lewis acid boron site and the subsequent incorporation of molecular oxygen forms an alkyl peroxy complex which is stabilized on the surface Lewis acid three-coordinated B sites. It desorbs as acetaldehyde. At high boron loading, crystalline boria is expected to dominate.

However, B-doped BPO_4 is unstable in the presence of water vapor above 823 K. Other elements, such as Mg-, Ca-, and Zn-doped BPO_4 are stable under water vapor above 823 K. These pure additives are less active than BPO_4, but the performance of Mg-, Ca-, and Zn-doped BPO_4 is comparable to B-doped BPO_4 [141]. These additives decrease the apparent activation energy of ethane and increase the selectivity of acetaldehyde at low surface coverage on BPO_4 substrate. The active site must be surface-interacting Mg, Ca and Zn species on the BPO_4 substrate. Quantum calculations show the effect of the element M (M=Mg, Ca, Zn) on the =B–O–M= bond. The addition of M affects the basicity of the oxygen ion near B and correlates with the decrease in the apparent activation energy of ethane [142].

2.6. Supported multicomponent oxides

The use of mixed oxide catalysts is a very versatile method to tailor the catalytic properties. Thorsteinson et al. showed its applicability for ethane oxidation using mixed oxides of V and Mo, together with other transition metal oxides. The MoVNb formulation appeared to be the most efficient for the production of ethylene and acetic acid from ethane [143]. These authors claimed a 50% conversion of ethane and a 68% selectivity of ethylene at 673 K. More recently, this catalytic system has been further examined by Burch et al. [144] and by Desponds et al. [145], focusing mainly on the relevance and role of Nb in the redox properties. The presence of a third element significantly improves the performance of the binary MoV catalyst. The advantages of Nb as a third component for ethane oxidation has recently been reported by Juárez-López et al. [146] for VSb-based multicomponent oxides. As in the former reports, the modification of redox properties and the possible formation of new mixed oxide phases are determining factors for the selectivity, while the presence of pure phases is detrimental for selective oxidation. The use of alumina-supported catalysts based on bulk MVNb (M=Co, Ni, Bi, Sn) has been reported [61,147]. The work by Valenzuela et al. stresses appropriate determination of catalyst reducibility, since TPR methodology evaluates bulk reduction and the reducibility of surface sites may not correspond to that of the bulk sites. Surface reducibility has been determined by XPS. Evaluation of alumina–supported NiV, NiVSb, and SbV oxides show that the selectivity of ethylene does not correlate with bulk reducibility, determined by TPR, but does correlate with surface reducibility, determined by XPS [61]. No interference from gas-phase reaction is expected, since the data were obtained below 773 K, and void volume was absent in the reactor. Accordingly, the results correspond to a pure catalytic process. Surface reducibility and ethylene selectivity follow the trend $NiVSb/Al_2O_3$>SbV/Al_2O_3>NiV/Al_2O_3, whereas bulk reducibility, as determined by TPR, follows the trend NiV/Al_2O_3>$NiVSb/Al_2O_3$>SbV/Al_2O_3. Relative activity follows the trend NiV/Al_2O_3–SbV/Al_2O_3>$NiVSb/Al_2O_3$, which does not correspond to surface or bulk reducibility.

2.7. Activation by Cl and Cl-containing catalysts

The methane molecule has been successfully activated using chlorine. As the rate of reaction of Cl with ethane is 600-fold higher than with methane [148], its relevance in ethane oxidation is expected to be remarkable. Additionally, Cl-promoted catalysts show very low activity as regards further oxidation of ethylene [149,150]. The use of organochloride additives increases the oxidation of ethane. Recently Hong

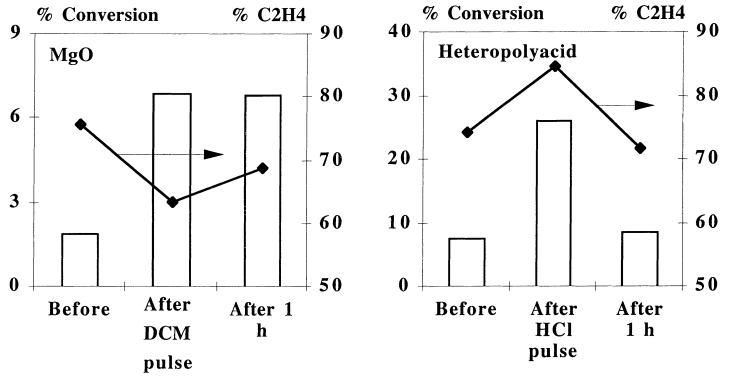

Fig. 3. Effect of HCl [2] or DCM [139] pulses on the reaction feed of ethane oxidation. Reaction conditions: [2], 743 K residence time, 3.5 s, C_2H_6:O_2:He=35:16:49; [151], pulses of 1100 ppm DCM on 20 mg, 923 K, total flow, 60 ml/min, C_2H_6:O_2:N_2=ca. 8:8:84.

and Moffat [62] have reported the effect of TCM for ethane oxidation on silica–supported 12-molybdophosphoric acid. Addition of TCM to the feed up to 0.4% mol increases conversion continuously, and selectivity remains largely unaffected; nearly 45% for acetaldehyde and 35% for ethylene. Surface Cl species appear to be formed and remain for some time in basic oxides [151], although this does not appear to be the case of heteropolyoxometallates [2]. Fig. 3 shows the selectivity of ethylene and the conversion of ethane before, just after, and after the pulse of Cl precursor (TCM or HCl). While MgO has higher activity after 1 h, this is not the case for $K_2P_{1.2}Mo_{10}W_1Sb_1Fe_1Cr_{0.5}Ce_{0.75}O_n$. Rare earth oxides show different trends under operation with TCM. La_2O_3, Sm_2O_3 or Pr_6O_{11} displays very moderate changes in the activity and ethylene selectivity. Some increase in the CO/CO_2 selectivity ratio results for Pr_6O_{11}, but CeO_2 is by far the most affected. At 773 K its activity almost doubles [152], and the selectivity of ethylene increases almost four times at the expense of CO_x species and the deep oxidation product, CO_2, is largely reduced.

The addition of DCM may also exert an effect in the homogeneous reaction, along with the surface modification of the catalysts. At high reaction temperatures (998–1098 K), where the gas-phase reaction appears to be dominant, no effect of the addition of DCM is observed, because the reaction conditions are sufficient to activate ethane and further activation by DCM may not be appreciable. Burch et al. [150] have shown that the addition of CH_3Cl has no effect of pure gas-phase oxidation of ethane with oxygen, leaving the effect of Cl to the modification of surface sites by interaction with chlorine species. Heteropolyacids may be affected only under Cl-feed. By contrast, this modification appears to be rather stable for magnesia and samaria. Hours after the organochloride promoter feed has been discontinued, activity remains high (ca. three times higher), indicating a possible modification of the surface of the catalyst and thus creating new sites essentially active and selective for ethane conversion [151]. Furthermore, the formation of a layer of $MnCl_2$ on K/Mn_2O_3 catalysts has been observed upon addition of chloroform to the reaction feed, under OCM reaction conditions [153]. Addition of DCM to the reaction feed for $Mg_3(PO_4)_2$ in the temperature range 723–823 K increased the selectivity of ethylene by a factor of 5 [75]. The promoting effect appears to be associated with the formation of chlorine compounds with Mg on the surface of the catalysts, as evidenced by the performance for ethane oxidation of $Mg_3(PO_4)_2$ catalysts pretreated in TCM and by the interaction of Cl with the catalysts evidenced by XPS measurements of the catalysts after reaction. In situ characterization under reaction conditions should provide a better understanding of the surface transformation of the catalysts under chlorine feed.

The chlorine-containing catalysts studied for methane oxidative coupling show very low activity for conversion of ethene vs. ethane [150,154]. Thus, a highly selective activity for ethane oxydehydrogenation would be expected. Additionally, the presence of chlorine in some catalysts triggers the reactivity.

However, their low long-term stability limits applicability and poses an environmental problem due to the release of chlorine from the catalyst. The benefits of the stabilization of the Cl-containing catalysts are evident and pass through the development of more stable structures and a moderation of the reaction conditions (temperature). Conway et al. evaluated Li–MgO–Cl materials as a support for several oxides [155] since these oxides have been reported to decrease the operation temperature [156]. The Cl/Li atomic ratio plays a key role, because Li stabilizes the Cl additive. For Cl/Li atomic ratios above 11, chlorine is lost until the ratio decreases to ca. 0.9–1. If the initial Cl/Li atomic ratio is 0.9 little chlorine is lost on stream. XPS measurements show that a LiCl layer is formed on top of the MgO support [157] as predicted by atomistic calculations [158]. The thin layer of Li_2O that appears to be formed on top of LiCl is expected to be the active phase. The catalyst Cl–Li–MgO with a Cl/L ratio of 0.9 is remarkably active, selective, and stable at 893 K, maintaining 58% yield of ethylene (75% conversion, 77% selectivity) over 50 h on stream [157]. The presence of oxides of Sn, La, Nd, and Dy results in a remarkable increase in conversion and at the same time maintains good selectivity of ethylene. The yield of ethylene is above 50%, although some deactivation is still evident.

Ueda et al. [159] have recently reported the performance of complex metal chloride oxides containing bismuth, alkali, alkaline earth, chlorine and oxygen. The presence of void volume in the reactor was minimized to prevent gas-phase reaction interference and blank tests showed no measurable activity. The catalyst studied possesses a layered structure comprising of $SrBi_3O_4Cl$ units, and is very active although its stability is low. Lead additive affords a very active catalyst but deactivates readily (Table 5). The addition of Sr promotes stability but conversion is lower. Among the formulations tested, the catalytic performance upon the addition of KCl and $SrCl_2$ resulted in a very active and stable $KSr_2Vi_3O_4Cl_6$ catalyst, with no structural modification measurable by XRD after 6 h on stream. However, a moderate degradation of the surface of the catalyst does appear to take place because some HCl is detected at the outlet of the catalyst. Li- and Na-promoted catalysts show very similar performance but structural degradation, although moderate, is observed in XRD experiments.

The use of other halogen additives is scarce, but very recently, F-promoted catalysts have been reported by Luo and Wan to reach 94.5% selectivity of ethylene at 23.4% conversion at 953 K on a LaF_3-promoted ceria catalyst [160]. However, the long term stability of the catalyst must be evaluated. A remarkable performance is presented by Au et al. [161] with a $BaBr_2/Ho_2O_3$ catalyst, which shows significant deactivation during the first 4 h of operation (from 88% selectivity of ethylene at 71% of conversion after 1 h on stream to 64% selectivity of ethylene at 52% conversion after 4 h on stream). Nevertheless, after this initial deactivation, the yield of ethylene remains essentially constant at 33% (64% ethylene selectivity at 52% conversion) during atleast 48 h on stream.

2.8. Non-reducible catalysts

The conversion of ethane on Li–doped magnesia is a heterogeneous–homogeneous catalytic process [53,54,140,162,163] due to its ability to generate ethyl radicals [53]. This strongly promotes selectivity since the oxidation of ethylene on LiMgO catalysts is non-selective [53,162]. As indicated by Burch and Crabb, there are quite a few reports about ethane ODH on non-reducible oxide catalysts; for example, LiNaMg

Table 5
Catalytic performance of layered metal chloride oxide [159]

Catalyst	Conversion (%)		Selectivity (%)			Yield (%) C_2H_4	Observations
			C_2H_4	CO	CO_2		
$PbBi_3O_4Cl_3$	51.4	81.5	87.6	4.3	8.1	45.0	Unstable
$SrBi_3O_4Cl_3$	19.5	31.7	89.4	2.5	8.1	17.4	Stable
$KSr_2Bi_3O_4Cl_6$	45.3	64.2	92.2	2.8	5.0	41.7	Very stable

Reaction conditions: 4 g, total flow 50 ml/min; C_2H_6:O_2:He=10:5:35, 933 K.

catalysts with an 86% selectivity of ethylene at a conversion of 38% at 898 K [164] or a selectivity of 46.3% at a conversion of 37.3% at 823 K on a Sn-based catalyst [165].

Non-reducible oxides for ethane oxidation run through a different mechanism than on reducible oxides, because redox functionality is absent. A heterogeneous–homogeneous reaction scheme where the oxide participates along with the homogeneous phase appears to be present. Thus, the oxidation of ethane on La_2O_3, Sm_2O_3, CeO_2, and Pr_6O_{11} points to a reactivity order per surface area unit like: $La_2O_3 > Sm_2O_3 \gg Pr_6O_{11} \sim CeO_2$. The selectivity of ethylene is one order of magnitude higher for the non-reducible oxides La_2O_3 and Sm_2O_3. Redox functionality promotes further non-selective oxidation [166]. For non-reducible oxides, such as Sm_2O_3, oxidation must occur on surface-activated oxygen species generated from the chemisorption of molecular oxygen [167]. Alkali-promoted La_2O_3, Sm_2O_3 and MnO_2 have fewer sites for total oxidation, thus accounting for the higher ethylene selectivity of the oxidative coupling of methane, which is also expected to be beneficial for ethane oxydehydrogenation [149,168].

As commented above, the addition of Cl improves both activity and selectivity (Table 6). The effect of different additives on the LiMgO catalyst was reported by Swaan at al. [81] who minimized the relevance of homogeneous gas-phase reaction. La and Ce oxides did not affect catalyst performance. The presence of Co and P, and mainly Na increased selectivity, but the catalyst was less active. Na minimized the formation of CO. The addition of Nb or Cu sharply decreased selectivity, with a lesser effect on activity while Co and Sn increased activity at the expense of the selectivity of ethylene [81].

2.9. Other catalytic formulations

Many oxides of elements of the first row of transition are active for total oxidation. However, some of these elements have been tested for the selective oxidation of ethane. Aika and coworkers have used a CoO/MgO catalyst for ethane oxidation with N_2O. The activation of N_2O is directly proportional to the number of surface Co^{2+} sites [64]. However, the authors report a low selectivity for ethylene. IR spectra after the reaction points to the existence of surface carbonates, formate and acetate species, even when no oxygenates are formed. The low selectivity of these catalysts results from the much higher (ca. 7 times) reactivity of the catalyst with ethylene than with ethane. Blaauw et al. [56] have also studied cobalt supported on silica and on saponite. The acid–base features of the support did not appear to have any effect for ethane ODH. However, the particle size of cobalt oxide is important, since Co aggregates show lower activity per exposed Co site. The interaction with the support, mainly in the layered structure of saponite, did influence selectivity, which was higher than for larger aggregates of cobalt oxide [56].

Table 6
Catalytic ethane oxidation on Li–Mg based supported oxides

Catalyst	Time (h)	Temperature (K)	Conversion (%) C_2H_6	Selectivity (%)					Yield (%) C_2H_4	References
				C_2H_4	CO	CH_4	CO_2	C_3+		
Li–Mg	–	898	53.9	63.8	6.4	1.9	22.3	0.9		[54]
Li–Mg–Cl	4.8	893	63.0	72.2	1.6	1.4	24.8	–	45.5	[155]
Sn/Li–Mg–Cl	4.8	893	78.7	71.6	2.1	1.0	24.0	1.2	56.4	[155]
Dy/Li–Mg–Cl	5.1	843	81.3	76.2	3.3	0.6	18.5	1.5	62.0	[155]
Li–Mg	–	854	38.0	79.7	4.2	0.0	15.0	–	30.3	[81]
Li–Na–Mg	–	898	38.0	86.4	1.4	0.2	11.7	–	32.8	[81]
Li–Co–Mg	–	823	20.0	70.5	1.2	0.2	28.4	–	14.1	[81]
Cl–Li–MgO (Cl/Li=0.9)	50	893	ca. 75	ca. 77	–	–	–	–	ca. 58	[157]

Reaction conditions: [54], C_2H_6/O_2 ratio=2/1, W=6.5 g, contact time, 12 s; [81], W=6.2 g, C_2H_6:O_2:He=12:6:82; [155,157], F=60 ml/min, 1 ml catalyst, $PC_2H_6+PO_2$=290+290 Torr.

The conversion of ethane on FeO^+ catalyst under nitrous oxide produces ethylene and ethanol [65]. FT ion cyclotron resonance reveals the existence of a common intermediate for the reaction products.

Chromium oxide has also been used for selective ethane oxidation. Loukah at al. [169] evaluated its performance when Cr is supported on silica, zirconia and modified zirconium phosphates. The specific support affects activity and Cr loading on the modified zirconium phosphate determines its structure and catalytic performance. Crystalline chromia is observed at high loading and this presents a total oxidation performance. The layered Zr phosphate incorporates Cr in its structure but some Cr sites may not be accessible, since the conversion is moderate. The best catalytic performance is achieved by $CrPO_4$, with 30% conversion and 60% selectivity of ethylene. Since the layered Zr–phosphate substrate has excess P at the surface, it is likely that P-coordinates chromia species be formed; these would account for the decrease in total oxidation for the layered Cr-based catalysts [169]. While crystalline chromia is a total oxidation site, its interaction with P promotes selectivity.

Chromium intercalated into ion-exchanged Na–montmorillonites has also been used for selective ethane oxidation by Olivera-Pastor et al. [170]. The resulting materials are stable up to 900 K with high surface coverage. For samples with moderate Cr loading, activity is strongly influenced by pretreatment of the catalyst, as this strongly influence the acidic properties of the materials [170].

Chang et al. [59] have evaluated ethane oxydehydrogenation on *ZSM-5 based* catalysts (H, Na, Ni, Pt, Ga, and V). Basic Na–ZSM-5 and neutral [V]–ZSM-5 perform better than acid H–ZSM-5 for the oxidative dehydrogenation of ethane. Addition of steam increases the selectivity to hydrocarbons since it reduces cracking to methane, reaching selectivity of ethylene of ca. 78% and conversion of ethane of ca. 43% at 823 K. No deactivation is observed up to 6 h on stream. However, Ga- and Ni-containing zeolites catalyze cracking and promote carbonaceous deposits, which is not desirable for oxidative dehydrogenation. However, they may be important for ethane aromatization.

2.10. New trends in selective ethane oxidation

The conversion of ethane to ethylene may become highly selective as ethylene is much less reactive than ethane with several catalysts. As the selective conversion of ethane to oxygenates is seriously limited due to the higher reactivity of C_2-oxygenates [36], high selectivities of C_2-oxygenates are only accomplished at low conversion levels. It is then necessary to look for alternative activation means than would allow the conversion of ethane in conditions which are not likely to degrade the oxygenates formed. As in the case of methane [171–173] the low-temperature conversion of ethane promotes oxygenates vs. hydrocarbons [33,123]. Thus the development of methods capable of activating ethane at lower temperatures would not only afford a lower tendency to degrade oxygenated products, but also increase the production of oxygenates to a larger extent. Several reports have been presented in this line.

2.10.1. Electrochemical activation of the oxidant

The electrochemical activation of oxygen on a Au/YSZ/Ag (YSZ, yttria-stabilized zirconia) electrochemical membrane system developed by Hamakawa et al. [174] shows that ethane oxidation is directly proportional to the activation of oxygen and that all the activated oxygen participates in the reaction. The use of gold layers prevents the chemical activation of oxygen, and permits an evaluation of the relevance of oxygen pumping upon application of a voltage in the cell. Acetaldehyde and CO_2 are the oxidation products under electrochemical conditions whereas CO_x and ethylene are formed under conventional conditions. This highlights the relevance of surface activated oxygen species and reaction temperature. The surface oxygen species is expected to be O^-, but no evidence has been reported in this sense [174].

The ability of YSZ to pump reactive oxygen through oxygen anion conduction has lead Otsuka et al. [175] to use it as a support for boria. Otsuka's work evaluates the catalytic performance of boria supported on YSZ [175]. Boria has proved to be active and selective for ODH on different supports [116,139]. B_2O_3/YSZ is active for ethane oxidation in an open circuit at 948 K. In a closed circuit, activated oxygen, which originates from the migration of oxide ions, is generated and activity increases with voltage, by a

factor of up to ca. 1.7 at 6 V. The active site appears to be associated with the boria–YSZ interface, and surface peroxide species have been proposed to be the active sites as determined by XPS. However, the binding energies reported are somewhat high [175].

2.10.2. Photocatalytic activation

Photocatalytic ethane oxidation has also been proposed as a very promising method to circumvent the low selectivity of thermal oxidation of alkanes with oxygen. The electrochemical method discussed above produces significant amounts of CO_x [116,174,175]. Partial oxidation of alkanes by UV-light is also affected by low selectivity due to the high energy of the photons [176–178]. The low selectivity in oxidation with O_2 is due to the very energetic conditions required to activate the reactants. UV-light assisted conversion activates oxygen through electron transfer for the alkane forming O_2^- and an alkyl cation, which readily releases a proton to form OOH radicals. Subsequent formation of the alkyl hydroperoxide may be followed by homolytic cleavage into highly reactive OH and alkoxy radicals, which further promote the non-selective degradation of partial oxidation products. However, photocatalytic oxidation at moderate temperatures, or even at room temperatures, is rather selective [179–181]. The photocatalytic oxidation of alkanes on oxides depends on the length of the hydrocarbon chain, as reported by Djeghri et al. [176]. The photoactivation of C_2 to C_8 hydrocarbons takes place on titania. Oxygenates are formed, but CO_2 is the dominant product. As in the case of thermal catalytic hydrocarbon oxidation, reactivity is affected by the type of carbon and decreases as follows: $C_{tert}>C_{quart}>C_{sec}>C_{prim}$ [176]. Some catalysts have recently been reported for the selective photooxidation of ethane to acetaldehyde. Wada et al. evaluated supported molybdena catalysts for ethane photooxidation [181,182]. ZnO–supported molybdena shows no measurable activity at 548 K without UV irradiation. MoO_3/ZnO is selective to acetaldehyde under UV irradiation at 493 K, but conversion is low (<1%) [182]. Formaldehyde and CO_2 are also formed to a significant extent. The ZnO support is more active and selective to acetaldehyde (selectivity 68%) but CO_2 formation is still considerable (24%). The situation is different for silica–supported molybdena catalysts [181]. No thermal activity is observed at 483 K. Conversion is still low under irradiation at 493 K, but acetaldehyde and formaldehyde are the main oxidation products, and minor amounts of CO_2 and ethanol are also formed [181]. Total activity increases with the temperature of the catalyst bed, but above 470 K acetaldehyde formation decreases and formaldehyde production increases. This suggests that formaldehyde might originate from further degradation of acetaldehyde, as in the conventional oxidation of ethane.

Recently, Frei and coworkers have used CaY and BaY zeolites to render complete selective photooxidation of ethane to acetaldehyde with O_2 under visible light [179,183,184]. Under their conditions, no CO_x byproducts were observed, acetaldehyde being the only oxidation product along with water. Under irradiation alkane radical cations are formed, as demonstrated spectroscopically, and tend to deprotonate to form alkyl radicals [185]. Under moderate reaction conditions, the alkyl hydroperoxide radical formed readily dehydrates in the zeolite environment, thus producing carbonyl products with no side reaction. The use of low energy photons and low temperature precludes homolysis of peroxide bonds, into very reactive alkoxy and hydroxy radicals, which would promote the non-selective attack to the partial oxidation products [180]. Pore sizes on the nm scale impose diffusional restriction on reaction intermediates, which is essential for high selectivity. In situ IR spectra show that acetaldehyde and water are the only products formed, even at the highest conversion (20%) [179]. This result clearly breaks the reported limiting yield of acetaldehyde under conventional reaction conditions. IR studies suggest that initially the intermediate ethylhydroperoxide species is formed. CaY zeolite affords a higher photochemical yield due to the higher electrostatic field inside the CaY cage, which increases the stabilization of the ethane O_2 charge transfer state [179].The electrostatic effect accounts for the activity order, which decreases thus: CaY> BaY$\gg$NaY (NaY is inactive). The participation of acid sites in CaY zeolites cannot be excluded. However, the high electrostatic field in the supercage of Ca–exchange Y zeolite has also been measured by EPR [186,187] and determined by model calculation [188]. The physical confinement imposed by the zeolite cage also prevents random radical reactions and the homolytic fragmentation of primary products,

hence increasing the selectivity. The oxidation by O_2 with Vis-light is extremely selective, and these systems have also been successfully applied to the oxidation of olefins, alkyls substituted benzenes, and other alkanes by O_2 in zeolites under Vis-light [179,183]. This latter group has just made a very stimulating review on complete selective oxidation reactions by O_2 under Vis-light in zeolites [180].

2.10.3. Activation by ozone

Ozone is a convenient radical initiator at moderate reaction temperatures. It decomposes into molecular oxygen and atomic oxygen. The latter is extremely reactive and reacts with alkanes to form alkyl radicals, thus initiating a radical reaction mechanism. Gesser et al. have reported the conversion of ethane to C_1- and C_2-oxygenates in the gas-phase with combined formaldehyde–methanol–acetaldehyde–ethanol selectivity between 36.7% and 95.7% at an ethane conversion equal or lower than 6.1% [189]. Li and Oyama have reported similar results for the selective gas-phase methane oxidation to formaldehyde using ozone as a radical initiator [190]. When a catalyst is present (Mg or Li/MgO), the reactivity is further improved [190]. The MgO catalyst is active for non-selective CO and CO_2 formation, whereas the Li/MgO catalyst promotes the production of formaldehyde. Consequently, the combined use of ozone and an appropriate catalyst is expected to significantly improve the production of oxygenates from ethane.

2.10.4. Activation by acids

Fe and Mn, supported on sulfated zirconia (SZ), have been used for the activation of ethane. These catalysts convert ethane to ethylene along with methane and butane at 573–673 K. Other acids, such as SZ, H–ZSM-5, or USY zeolite show no activity at all at this temperature. At a higher temperature (723 K), these solid acids also activate ethane. The initial selectivity of ethylene at 0.1% conversion is close to 98%, 94%, 97%, and 99% for SZ, FeMn/SZ, H–ZSM-5, and USY zeolite, respectively. The observed mechanism is analogous to that seen in superacid solutions [191,192]. The FeMn/SZ catalyst has the highest acidity in the series [193,194] since it runs at lower temperature than conventional solid catalysts.

2.10.5. Monolithic reactors

The use of monolithic catalysts for the production of ethylene or syngas from ethane has been reported by Schmidt and coworkers [195–197] for supported noble metal. The application of supported oxide should be a highly attractive option because of the high space velocities that can be reached.

2.10.6. Membrane reactors

A certain increase in the yield of ethylene has been achieved with membrane reactors. A membrane reactor alters the thermodynamic equilibrium of chemical reactions. Oxygen can be permeated through the membrane that would provide stoichiometric hydrocarbon-to-oxygen levels along the membrane. This configuration prevents high local oxygen concentration [198,199]. Alumina-based membrane reactors have been used to support Li/MgO catalysts [198,199] and SmO/MgO catalysts [199] as active phases for selective ethane ODH. Membrane reactors show better performance than conventional ones in both yield and selectivity at low feed ratios. This difference decreases as feed ratios increase [198]. At low ethane-to-oxygen ratios, the ethylene yield is close to 50% [198]. Mixed membrane reactors, equivalent to a membrane reactor followed by a conventional fixed bed reactor, yield 57% ethylene [199].

3. Aromatization of ethane

The production of BTX (benzene, toluene and xylene) hydrocarbons from LPG should significantly reduce the cost of these hydrocarbons, which are mainly produced by the reforming of naphthas. The feedstock of naphthas accounts for ca. 80% of the production cost of BTX [200] and references therein. The conversion of paraffins to aromatics has essentially been achieved from propane and larger hydrocarbons [200–203]. For instance, *n*-butane is 100 times more reactive than ethane [204]. Methane and ethane are harder to convert to BTX hydrocarbons [201]. Actually, methane is formed as a byproduct of the cracking of hydrocarbons and does no undergo secondary transformations under aromatization reaction conditions [203–205]. The presence of strong acid sites promotes the formation of methane [206]. Despite the considerable interest in the aromatization

of ethane since the original patent by Chu [207], only few papers addressing this have appeared in the literature in the last 10 years. Alkanes appear to be activated as in superacid solutions [191] but at higher temperatures, through protolysis of their C–H or C–C bonds, which finally result in olefins. These undergo further transformation, such as oligomerization, cracking, cyclization of oligomers, and aromatization. The yields of the products vs. contact time show that ethylene is the main product at low residence times. The conversion of alkanes to aromatics takes advantage of the molecular confinement provided by the structure of zeolites, which affects product distribution. However, deactivation by coking is important and certain characteristics should also be present in the zeolite. Most research has therefore been carried out on ZSM-5 zeolite, which has an intermediate pore and channel size [208], which limits the formation of large polynuclear aromatics, that lead to coke formation. These zeolites present high acidity [204] but the acid sites are separated. This is an important condition since close acid sites promote coke formation [201,209]. The use of metals has a promoting effect, which is affected by its dispersion and the use of other additives [200,208,210–215]. However, catalysis by metals is out of the scope of this review. The use of Zn or Ga slows down the deactivation by coke [3,151,217]. Aromatization is promoted by Zn and Ga [145,211,215–217]. The presence of Zn or Ga in modified H–ZSM-5 zeolites increases ethane conversion from 2% on H–ZSM-5 to 52% on Zn–H–ZSM-5. Ga has intermediate activity [203]. However, under reducing conditions (such those imposed by aromatization), Zn can be eluted from the zeolite, while Ga undergoes a much less intense elution due to its much higher boiling point [201,218]. In fact, Ga increases stability on stream beyond 15 h [3], because it is highly stable under redox cycles [201]. The presence of Ga or Zn species increases the initial formation of olefins, which appears to be the rate-determining-step [204]. A bifunctional mechanism appears to take place on Ga-containing zeolites: (1) dehydrogenation in the Ga sites, and (2) oligomerization and dehydrociclyzation in the protonic sites [208]. Acid zeolites, such as H–ZSM-5, convert light alkanes into aromatics. However, the aromatization also yields light alkanes, since it occurs accompanied by cracking, thus limiting yield [203,215,219]. Oligomerization appears to take place on acidic sites; these alkenes must subsequently be dehydrogenated to aromatics. Evidence has been presented that both Zn and acidic sites must be present [203,215]

Recent work by Bandeira and Taârit provides kinetic evidence that the initial dehydrogenation of ethane and subsequent oligomerization and dehydrocyclization are associated with the same active site. Thus, the reactants and intermediates compete for the same site [220]. A similar conclusion has been reached by Haagen et al. in transient studies on H–ZSM-5 and Zn–H–ZSM-5 [221]. Ethane pulses at 773 K forms ethylene on H–ZSM-5. A continuous feed of ethylene, the primary product, yields alkyl aromatics on H–ZSM-5 and benzene on Zn–H–ZSM-5. It therefore appears that Zn species are not only essential in the activation of the ethane molecule but also in subsequent reactions to aromatics [221]. Thus, reactants and intermediates could compete for the Zn site. It is interesting to note that the relevance of acid sites under pulse conditions is not significant, since the experiments afford comparable results for Zn–H–ZSM-5 and Zn–Na–ZSM-5. However, at longer reaction times, Brønsted sites must participate, as suggested by the formation of isobutene, and subsequently, alkyl aromatics. However, the Al content does not linearly correlate with activity [3], suggesting that it is not only acidity that promotes activity.

Schultz and Baerns have observed that ethane is dehydrogenated on both Ga_2O_3 outside the surface of zeolites and on their acid sites [3], in agreement with IR studies by Yakerson et al. [222]. The BTX yield increases linearly with Ga contents up to 3 wt% and then levels off. However, the need for exchanged Ga^+ cations in the zeolite lattice has been observed by several authors and their presence is associated with better aromatization performance [223–227]. The lower reactivity of a physical mixture of Ga_2O_3+H–ZSM-5 vs. impregnated or ion exchanged Ga_2O_3/H–ZSM-5 highlights the relevance of Ga dispersion in the zeolite (Fig. 4). However, it has been reported that the dehydrogenation activity of the framework Ga atoms is lower than that of the extra-framework gallium species [200,228,229]. Several results reviewed by Seddon [201] and Guisnet et al. [200] support the relevance of non-framework Ga species strongly interacting with zeolite. In fact, the

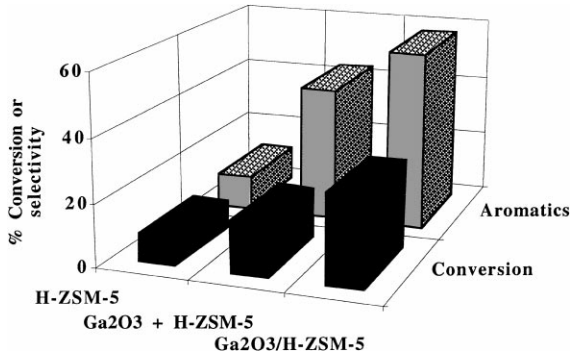

Fig. 4. Ethane conversion of H–ZSM-5 zeolite (SI/Al ratio, 15), pure, mixed with Ga_2O_3 and impregnated with Ga_2O_3. Reaction conditions: 873 K; 18.8<20.5 gh/mol [3].

dispersion of Ga appears to account for the activation of the catalyst on stream [225,230] since the H_2 released may promote the reduction and dispersion of the Ga species. Dispersed Ga species close to acid sites appear to be critical for catalyst performance. However, they may be not integrated in the framework, but rather highly dispersed in the pore structure. The formation of a highly dispersed reduced Ga species has been observed with K-edge X-ray absorption spectroscopy during on stream operation and with ^{71}Ga-MAS-NMR by Meitzner et al. [231]. The species, probably GaHx, appears to be formed during the reaction. This is an example of the relevance of in situ characterization under reaction conditions. The use of other H acceptors like Zr_2Fe results in a 5-fold higher yield of aromatics on Zn–, Ga– and Pt–CVM pentasils (similar to H–ZSM-5) [232].

The relevance of redox and acid sites for ethane oxidative dehydrogenation on other microporous materials (APO-5) has been proposed by Concepción et al. [109]. Despite their lower stability, Mo and W have also been used on H–ZSM-5 zeolites (Si/Al 50) for the conversion of ethane. Mo/H–ZSM-5 is more active than W/H–ZSM-5. The formation of Mo_2C is proposed to afford for the good performance of molybdena-based catalysts [233]. The cracking to methane is significant for all catalysts, but production of BTX is also important. W/H–ZSM-5 is highly selective but less active. The binary MoW/H–ZSM-5 catalyst is reported to show better activity and stability than single Mo- or W-supported catalysts [234].

4. Total oxidation of ethane

The total oxidation of ethane has been studied to a much lesser extent than the former reactions. Kinetic isotopic or in situ IR studies have demonstrated that the total and partial oxidation of ethane is initiated by the C–H bond cleavage of the weakest C–H bond in the molecule. The next step is the formation of surface oxygen-containing intermediates on an oxide catalyst. The reactivity of the catalyst and the stability of the intermediates will determine the selectivity profile. Precious metals have been used for the combustion of ethane more often than oxides [235–238]. However, the use of supported metal oxides is mainly focused on Cr and Cu. The activity of Cr oxide was reported by Yu Yao on Cr_2O_3 microcrystals [239]. Kinetic isotopic effect [239] and IR [240] indicate that the initial activation of the C–H bond is involved in the rate-controlling step for the oxidation of ethane, but not for ethylene. Ethylene appears to adsorb through the double bond, whose attack should be the rate-determining step [239,240]. The use of chromium oxide on titania, produces mainly CO_2 (ca. 96%) and little amount of ethylene [241]. Activity increases with chromia loading on titania, while selectivity values remain unaltered (Table 7). Apparently, titania support only serves to increase the exposure of chromia.

In situ studies of the total oxidation of ethane on $MgCr_2O_4$ by IR spectroscopy point to the formation of surface acetate species at 423 K. A weak band at 1385 cm^{-1} and a shoulder near 1580 cm^{-1} reveal the formation of traces of formate ions [242], pointing to profound oxidation. Other bands suggest the existence of dioxy-ethylydene species and surface acetaldehyde [242]. The latter species disappear upon further heating. Acetate species burn in the 573–773 K temperature range to produce CO_2 and water. The combustion of ethane appears to run via surface

Table 7
Oxidation of ethane on Cr_2O_3/TiO_2 [241]

Cr/(Cr+Ti) atomic ratio	Ethane conversion (%)	CO_2 selectivity (%)	C_2H_4 selectivity (%)
0.05	ca. 3	ca. 96	ca. 4
0.20	ca. 9	ca. 96	ca. 4
1.00	ca. 14	ca. 96	ca. 4

Reaction conditions: air/ethane: 2/1. Reaction temperature 723 K.

acetate species and acetaldehyde appears to be an earlier intermediate. In contrast with large hydrocarbons, no evidence of surface alkoxy species from ethane was observed by Finocchio et al., although the high temperature required to activate ethane may account for its ready oxidation to carbonyl groups [242]. It appears that the breaking of the weaker C–H bond is followed by the formation of a C–O bond. The results suggest that the observed acetate species are the final intermediates. Also, selective and non-selective oxidation reactions appear to be consecutive, as supported by the formation of partial oxidation products on the surface of combustion catalysts. The formation of these surface species has been observed in the absence of gas-phase oxidant, which aims to conclude that the total oxidation of oxides is not only consecutive to partial oxidation, but also that nucleophilic oxygen species (lattice oxygen) are also involved in total oxidation, if its binding energy is low enough. The selectivity-determining step proposed by Kung and coworkers [42,43] should be the relative rate of desorption of the partial oxidation products as compared to the reactivity of the oxygen species. Lee et al. have reported the relevance of lattice oxygen for total oxidation on a perovskite catalyst ($LaMnO_x$) using alternating pulses of ethane and oxygen [243]. These authors also show that surface hydrocarbon species remain on the surface for several minutes at 648 K between oxygen pulses.

The relevance of electrophilic oxygen proposed by Bielanski and Haber [244] does not contradict the former results, which highlight the relevance of nucleophilic oxygen for total oxidation, but provide no evidence to rule out the role of electrophilic oxygen species for combustion. It therefore appears that electrophilic oxygen species are associated with non-selective oxidation while nucleophilic oxygen species may be associated with selective and non-selective oxidation reaction. A transient kinetic study by Papageorgiou et al. on the reactivity of lattice (in the absence of gaseous oxygen) and adsorbed oxygen (in the presence of gaseous oxygen) species in the oxidation of ethane and ethylene, shows that both oxygen species are active for total oxidation on a Li^+/TiO_2 catalyst [245]. Lattice oxygen is a total oxidation site for ethane and ethene, reactivity being higher for the paraffin than for the olefin. Conversely, the reactivity trend is reversed for surface oxygen species. The relative activities of lattice and surface oxygen are affected by the loading of Li cation [245].

Cu-based catalysts are also used for ethane combustion. Kucherov and coworkers have reported that the complete oxidation of ethane on Cu–H–ZSM-5 catalyst correlates with the number of coordinately unsaturated square-planar cupric cations stabilized in ZSM-5 channels [246]. Only CO_2 and water are the oxidation products. However, the square planar Cu^{2+} species tend to irreversibly rearrange into isolated mono-cationic species by steam treatment at 903 K over 17 h, as observed with in situ EPR by Kucherov et al. [247]. These Cu species are exposed to the gas-phase molecules, but their activity decreases remarkably. The addition of La, or Ce appears to stabilize active square planar Cu^{2+} species [247]. Doping by

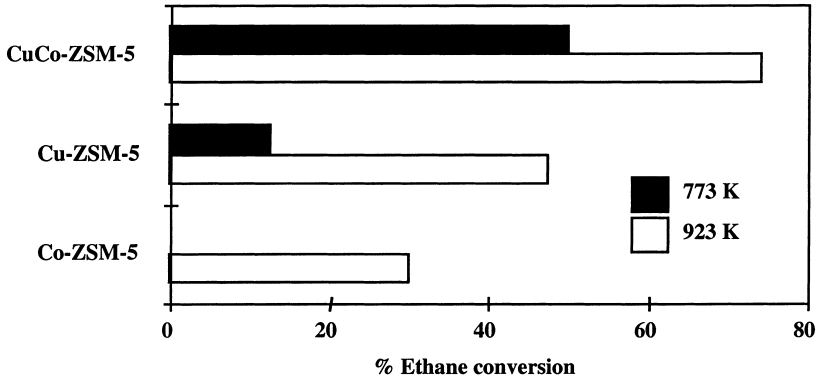

Fig. 5. Ethane total oxidation on ZSM-5-supported catalysts calcined at 773 and 923 K. Reaction conditons: $He+O_2+C_2H_6$=90.6+8.4+0.96 vol%. Space velocity, 20 000 h^{-1}. Reaction temperature, 673 K [248].

Co increases ethane oxidation activity (Fig. 5) [247,248]. The use of rare earth additives provides a significant stabilization to Cu–H–ZSM-5 based catalysts for ethane combustion. Co–H–ZSM-5 has an activity slightly lower than Cu–H–ZSM-5, but both catalysts deactivate under high temperature treatment. The Cu–Co–H–ZSM-5 catalyst is not only less sensitive to high temperature treatment, but also three times more active than monocationic catalysts (Fig. 5) [248]. The remarkable effect of cobalt requires that it must be in intimate interaction with Cu to improve its specific activity or the number or active sites. This interaction must also account for the high thermal stability of the bicationic catalyst. The support has no activity for the oxidation of ethane. However, if oxygen is replaced by N_2O the activity of the zeolite and Cu–H–ZSM-5 are comparable [249], but coke formation is significant near 673 K. The ability of Cu species to decompose N_2O decreases upon treatment at 723 K, but the oxidation of ethane remains unaffected [249]. The use of N_2O instead of O_2 changes the nature of the reaction mechanism, since it has a heterogeneous–homogeneous nature [249].

5. Conclusions

The results presented above show that the conversion of ethane is a new challenge in catalytic oxidation, which in the case of certain products can be run at reasonable yields. The dehydrogenation of ethane affords good selectivity. For this reaction the nature of the support oxide has a remarkable effect on the activity and selectivity of the supported metal oxide. Its relevance is related to modification of the Metal–O–support bond, which appears to be the most critical one for activity under oxidation conditions, since activity is altered near one order of magnitude. Redox and acid–base properties are strongly affected by the support. Whereas activity depends on the reducibility of the supported oxide, this does not appear to correlate with its oxidation state under reaction conditions. The presence of additives has a strong effect on activity; by contrast, the effect of surface coverage below monolayer loading values is only moderate. Structural knowledge about the effect of additives on supported oxides is still poor as regards the catalytic implications of structural, redox and acid–base modifications and further research must be done to understand the role of the additives. On the other hand, the conversion of ethane to C_2-oxygenates affords significantly lower yields under conventional catalyst formulation and reaction conditions. Since the production of C_2-oxygenates from ethane, mainly acetic acid, is a very attractive reaction for the industry it is necessary to develop new catalytic concepts that will allow the production of oxygenates with high yield, like new catalysts formulations, the use of different oxidants (nitrous oxide) or the application of alternative activation (electrochemical activation, photoactivation, reductant activation or radical initiators). Any advance in decreasing the reaction temperature will favor the selectivity and the formation of oxygenates. The use of radical initiators has afforded very attractive results for methane conversion, and could be of great use for ethane conversion. The use of chlorine-precursors in the gas-phase appears to result in a new Cl-containing surface catalyst structure, rather than affecting gas-phase reactivity, and yields higher conversions with comparable selectivity values; however, the stability on stream is low. While some results presented above indicate significant improvements in the stability of the halogen-containing catalysts, more effort should be directed to developing stable phases. The aromatization of ethane displays a different dependence on the support since it should present acidic sites and must prevent coke formation. The structure of the sites under aromatization reactions is significantly modified by reducing conditions. Gas-phase reactions may also play an important role, mainly at high temperature, when the ODH reaction is promoted. Chlorine-containing catalysts afford very high yields for ethane ODH, but in most cases stability is low. In situ characterization techniques should provide knowledge at molecular level about the catalytic site under oxidative and aromatization conditions, thus enabling the design of more efficient catalysts. Accordingly, it is foreseen that much future research will focus on molecular understanding of the catalyst during reaction. The nature of the oxidant determines catalytic performance since its interaction with the active site is determined by different parameters, molecular oxygen being more sensitive to redox properties, whereas nitrous oxide is subject to different requirements. The use of new technologies provides alternative means to promote activation of

ethane or the oxidant that will not lead to further degradation of partial oxidation products. Some of these new techniques have already afforded very promising results.

The need to control the reaction calls for control of the catalyst and of the catalytic systems. It is important to stress the relevance of molecular knowledge of the active site and its modifications under the reaction conditions. The emergence of new concepts to yield more efficient and selective activation includes the development of new catalysts and the use of alternative means to activate the hydrocarbon in such a way that the degradation of the desired product will be prevented. There are indeed many opportunities for development in ethane conversion that should afford a better production of olefins, oxygenates and aromatics.

Acknowledgements

This review is dedicated to Prof. J.L.G. Fierro and Prof. I.E. Wachs, who showed me how attractive catalysis is.

References

[1] G. Centi, F. Trifirò, Catal. Today 3 (1988) 151.
[2] F. Cavani, M. Koutyrev, F. Trifirò, Catal. Today 28 (1996) 319.
[3] P. Schulz, M. Baerns, Appl. Catal. 78 (1991) 15.
[4] M.S. Scurell, Appl. Catal 32 (1987) 1.
[5] R.D. Roark, S.D. Kohler, J.G. Ekerdt, Catal. Lett. 16 (1992) 71.
[6] C. Rocchiccioli-Deltcheff, M. Amirouche, M. Che, J.M. Tatibouët, M. Fournier, J. Catal. 125 (1990) 591.
[7] N. Das, H. Eckerdt, H. Hu, H.F. Walzer, F.J. Feher, I.E. Wachs, J. Phys. Chem. 97 (1993) 8240.
[8] H. Hu, I.E. Wachs, S.R. Bare, J. Phys. Chem. 99 (1995) 10897.
[9] M.A. Vuurman, I.E. Wachs, J. Phys. Chem. 96 (1992) 5008.
[10] F.J. Gil-Llambias, A.M. Escudei, J.L.G. Fierro, A. López Agudo, J. Catal. 95 (1985) 520.
[11] J.M. Stencel, J.R. Diehl, J.R. D'Este, L.E. Makovsky, L. Rodrigo, K. Marcinkowska, A. Adnot, P.C. Roberge, S. Kaliaguine, J. Phys. Chem. 90 (1986) 4739.
[12] K. Marcinkowska, L. Rodrigo, S. Kaliaguine, P.C. Roberge, J. Mol. Catal. 33 (1985) 189.
[13] I.E. Wachs, G. Deo, J. Phys. Chem. 95 (1991) 5889.
[14] M.A. Bañares, X. Gao, J.L. Fierro, I.E. Wachs, to be published.
[15] I.E. Wachs, J.-M. Jehng, G. Deo, B.M. Weckhuysen, V.V. Guliants, J.B. Benziger, Catal. Today 32 (1996) 47.
[16] I.E. Wachs, J.M. Jehng, G. Deo, B.M. Weckhuysen, V.V. Guliants, F.B. Benziger, S. Sundaresan, J. Catal. 170 (1997) 75.
[17] M.A. Bañares, N.D. Spencer, M.D. Jones, I.E. Wachs, J. Catal. 146 (1994) 204.
[18] M.A. Bañares, X. Gao, J.L.G. Fierro, I.E. Wachs, in: R.K. Grasselli, S.T. Oyama, A.M. Gaffney, J.E. Lyons (Eds.), Third World Congress on Oxidation Catalysis, Stud. Surf. Sci. Catal. 110 (1997) 295.
[19] I.E. Wachs, Catal. Today 27 (1996) 437.
[20] M.A. Bañares, H. Hu, I.E. Wachs, J. Catal. 155 (1995) 249.
[21] C. Rocchiccioli-Deltcheff, M. Amirouche, M. Che, J.M. Tatibouët, M. Fournier, J. Catal. 125 (1990) 292.
[22] A. Galli, J.M. López Nieto, A. Dejoz, M.I. Vazquez, Catal. Lett. 34 (1995) 51.
[23] G. Deo, I.E. Wachs, J. Catal. 146 (1994) 335.
[24] G. Ramis, G. Busca, F. Bregani, Catal. Lett. 18 (1993) 299.
[25] I.E. Wachs, B.M. Weckhuysen, Appl. Catal. A 157 (1997) 67.
[26] I.E. Wachs, G. Deo, B.M. Weckhuysen, A. Andreini, M.A. Vuurman, M. de Boer, M.D. Amiridis, J. Catal. 161 (1996) 211.
[27] M.A. Vuurman, D.J. Stufkens, Ad Oskam, G. Deo, I.E. Wachs, J. Chem. Soc. Faraday Trans. 92 (1996) 3259.
[28] L. Owens, H.H. Kung, J. Catal. 148 (1994) 587.
[29] A. Erdöhelyi, F. Máté, F. Solymosi, J. Catal. 135 (1992) 563.
[30] A. Erdöhelyi, F. Solymosi, Appl. Catal. 39 (1988) L11–L14.
[31] A. Erdöhelyi, F. Solymosi, J. Catal. 129 (1991) 497–510.
[32] M.A. Bañares, H. Hu, I.E. Wachs, J. Catal. 150 (1994) 407.
[33] S. Albonetti, F. Cavani, F. Trifirò, Catal. Rev.-Sci. Eng. 38 (1996) 413.
[34] F. Cavani, F. Trifirò, in: R.K. Grasselli, S.T. Oyama, A.M. Gaffney, J.E. Lyons (Eds.), Third World congress on Oxidation Catalysis, Stud. Surf. Sci. Catal. 110 (1997) 19.
[35] V.D. Sokolovskii, Catal. Today 24 (1995) 377.
[36] C. Batiot, B.K. Hodnett, Appl. Catal. A 137 (1996) 179.
[37] R. Burch, S.C. Tsang, Appl. Catal. 65 (1990) 259.
[38] G. Busca, E. Finochio, G. Ramis, G. Ricchiardi, Catal. Today 32 (1996) 133.
[39] P. Concepción, A. Galli, J.M. López Nieto, A. Dejoz, M.I. Vazquez, Topics Catal. 3 (1996) 451.
[40] P.M. Michalakos, M.C. Kung, I. Jahan, H.H. Kung, J. Catal. 140 (1993) 226.
[41] J.B. Moffat, Appl. Catal. A 146 (1996) 65.
[42] H.H. Kung, P. Michalakos, L. Owens, M. Kung, P. Andersen, O. Owen, I. Jahan, Catalytic selective oxidation, ACS Symp. Ser. 523 (1993) 389.
[43] H.H. Kung, Adv. Catal. 40 (1994) 1.
[44] T. Blasco, A. Galli, J.M. López Nieto, F. Trifirò, J. Catal. 169 (1997) 203.
[45] G.J. Hutchings, Selective oxidation of light alkanes, in: E.G. Derouane, J. Haber, F. Lemos, F.R. Riberiro, M. Guisnet (Eds.), Catalytic Activation and Fuctionalisation of Light Alkanes. Advances and Challenges, NATO ASI Series, Kluwer Academic Publishers, Dordrecht, 1998.

[46] A. Ekstrom, J.A. Lapszewicz, J. Phys. Chem. 93 (1989) 5230.
[47] L.M. Madeira, R.M. Martín-Aranda, F.J. Maldonado-Hódar, J.L.G. Fierro, M.F. Portela, J. Catal. 169 (1997) 469.
[48] R. Grabowski, B. Gryzbowska, A. Kozlowska, J. Sloczynski, K. Wcislo, Y. Barbaux, Topics Catal. 3 (1996) 277.
[49] Y.F. Chang, G.A. Somorjai, H. Heinemann, J. Catal. 154 (1995) 24.
[50] Ch.Y. Kao, K.T. Huang, B.Z. Wan, Ind. Eng. Chem. Res. 33 (1994) 2066.
[51] J. le Bars, A. Auroux, M. Forissier, J.C. Vedrine, J. Catal. 162 (1996) 250.
[52] E.N. Voskeresenkaya, V.G. Roguleva, A.G. Anshits, Catal. Rev.-Sci. Eng. 37 (1995) 101–143.
[53] Y. Ng Lee, F. Sapiña, E. Martínez, J.V. Folgado, V. Cortés Corberán, in: R.K. Grasselli, S.T. Oyama, A.M. Gaffney, J.E. Lyons (Eds.), Stud. Surf. Sci. Catal. 110 (1997) 747.
[54] E. Morales, J.H. Lunsford, J. Catal. 118 (1989) 235.
[55] R. Burch, E.M. Crabb, Appl. Catal. A 97 (1993) 49.
[56] R.J. Blaauw, Catalysts for the selective oxidation of ethane to ethylene, Ph.D. Dissertation, University Utrecht, Netherlands, 1997.
[57] G.A. Martin, A. Bates, V. Ducarme, C. Mirodatos, Appl. Catal. 47 (1989) 287.
[58] G. Mestl, P. Ruiz, B. Delmon, H. Knözinger, J. Phys. Chem. 98 (1994) 11269.
[59] Y.-F Chang, G.A. Somorjai, H. Heinemann, Appl. Catal. A 96 (1993) 305.
[60] R.Q. Long, Y.P. Huang, H.L. Wan, J. Raman Spectrosc. 28 (1997) 29.
[61] R.X. Valenzuela, J.L.G. Fierro, V. Cortés Corberán, E.A. Mamedov, Catal. Lett. 40 (1996) 223.
[62] S.S. Hong, J.B. Moffat, Catal. Lett. 40 (1996) 1.
[63] M.B. Ward, M.J. Lin, J.H. Lunsford, J. Catal. 50 (1977) 306.
[64] K.-I. Aika, M. Isobe, K. Kido, T. Moriyama, T. Onishi, J. Chem. Soc., Faraday Trans. 83 (1987) 3139.
[65] D. Schröder, H. Schwarz, Angewandte Chemie 29 (1990) 1431.
[66] Y. Wang, K. Otsuka, J. Catal. 171 (1997) 106.
[67] M.Yu. Sinev, V.N. Korchak, O.V. Krylov, Kinet. Catal. 30 (1989) 860.
[68] K.-I. Aika, J.H. Lunsford, J. Phys. Chem. 81 (1977) 1393.
[69] M.A. Bañares, J.L.G. Fierro, J.B. Moffat, J. Catal. 142 (1993) 406.
[70] T.-J. Yang, J.H. Lunsford, J. Catal. (1979) 505.
[71] A. Erdöhelyi, F. Solymosi, J. Catal. 123 (1990) 31.
[72] N.I. Ilchenko, W. Hanke, L.N. Rayevshatya, G.I. Golodets, G. Öhlamann, React. Kinet. Catal. Lett. 41 (1990) 147.
[73] N.I. Ilchenko, L.N. Rayevskaya, G.I. Golidets, W. Hanke, G. Ohlmann, Kinet. Katal. 33 (1992) 560.
[74] V.D. Sokolovskii, Catal. Rev.-Sci. Eng. 32 (1990) 1.
[75] S. Sugiyama, N. Kindo, K. Satomi, H. Hayashi, J.B. Moffat, J. Mol. Catal. A 95 (1995) 35.
[76] G. Colorio, J.C. Védrine, A. Auroux, B. Bonnetot, Appl. Catal. A 137 (1996) 55.
[77] P.M. Witt, L.F. Schmidt, J. Catal. 163 (1996) 465.
[78] J.H. Lunsford, E. Morales, D. Dissanayake, Ch. Shi, Int. J. Chem. Kinet. 26 (1994) 921.
[79] R. Rota, A. Servida, S. Carra, Ind. Eng. Chem. Res. 33 (1994) 2540.
[80] P. Dagaut, M. Cathonnet, J.-C. Boettner, Int. J. Chem. Kinet. 23 (1991) 437.
[81] H.M. Swann, A. Toebes, K. Seshan, F.G. van Ommen, F.R.H. Ross, Catal. Today 13 (1992) 629.
[82] S.T. Oyama, A.M. Middlebrook, G.A. Somorjai, J. Phys. Chem. 94 (1990) 5029.
[83] J.-M. Jehng, G. Deo, B.M. Weckhuysen, I.E. Wachs, J. Mol. Catal. A 110 (1996) 41.
[84] V.M. Vorotyntsev, V.A. Shvets, V.B. Kazansky, Kinet. Katal. 12 (1971) 1249.
[85] G. Deo, I.E. Wachs, J. Haber, Crit. Rev. Surf. Chem. 4 (1994) 141.
[86] G. Bond, S. Flamerz Tahir, Appl. Catal. 1 (1991).
[87] E.A. Mamedov, V. Cortés Corberán, Appl. Catal. A 127 (1995) 1.
[88] C. Hallett, BP European Patent, 0 480 594 A2 (1992).
[89] M. Kitson, BP European Patent, 0 407 091 A1 (1991).
[90] P. Barthe, European Patent, 0 479 692 A1 (1992).
[91] F. Trifirò, P. Centola, I. Pasquon, J. Catal. 10 (1968) 86.
[92] G. Busca, G. Centi, J. Am. Chem. Soc. 111 (1989) 46.
[93] J. Haber, Theoretical basis of the activation of the C–H bond, in: E.G. Derouane, J. Haber, F. Lemos, F.R. Riberiro, M. Guisnet (Eds.), Catalytic Activation and Fuctionalisation of Light Alkanes. Advances and Challenges, NATO ASI Series, Kluwer Academic Publishers, Dordrecht, 1998.
[94] G. Deo, I.E. Wachs, J. Catal. 146 (1994) 323.
[95] S.M. Aliev, V.d. Sokolovski, A.N. Startsev, B.N. Kusnetzov, React. Kinet. Catal. Lett. 22 (1983) 133.
[96] M.E. Lashier, G.L. Schrader, J. Catal. 128 (1991) 113.
[97] L.C. Glaeser, J.F. Bradzil, M.A. Hazle, M. Mehicic, R.K. Graselli, J. Chem. Soc., Faraday Trans. 1 81 (1985) 2903.
[98] M.A. Chaar, D. Patel, M.C. Kung, H.H. Kung, J. Catal. 105 (1987) 483.
[99] C.-B. Wang, G. Deo, I.E. Wachs, J. Catal. 178 (1998) 640.
[100] Z. Dang, J. Gu, J. Lin, D. Yang, Catal. Lett. 54 (1998) 129.
[101] I.E. Wachs, G. Deo, D.S. Kim, M.A. Vuurman, H. Hu, in: L. Guczi, F. Solymosi, P. Tétényi (Eds.), New Frontiers in Catalysis, Stud. Surf. Sci. Catal. 75 (1993) 543.
[102] S. Bordoni, F. Catellani, F. Cavani, F. Trifirò, M.P. Kulkarni, in: V. Cortés Corberán, S. Vic Bellón (Eds.), Second World Conference on Selective Oxidation, Stud. Surf. Sci. Catal. 82 (1994) 93.
[103] M.A. Bañares, L.J. Alemany, M. Carmen Jiménez, M.A. Larrubia, A. Martínez-Arias, F. Delgado, J.M. Blasco, M. López Granados, J.L.G. Fierro, J. Solid State Chem. 124 (1996) 69.
[104] L.J. Alemany, M.C. Jiménez, M.A. Bañares, J.M. Blasco, Mater. Res. Bull. 31 (1996) 513.
[105] R.Y. Saleh, I.E. Wachs, S.S. Chan, C.S. Chersich, J. Catal. 98 (1986) 102.
[106] G. Deo, A.M. Turek, I.E. Wachs, T. Machej, J. Haber, N. Das, H. Eckert, A.M. Hirt, Appl. Catal. A 91 (1992) 27.

[107] P. Concepción, A. Corma, J.M. López-Nieto, J. Pérez-Pariente, Appl. Catal A 143 (1996) 17.
[108] O.S. Owen, H.H. Kung, J. Mol. Catal. 79 (1993) 265.
[109] P. Concepción, J.M. López Nieto, A. Mifsud, J. Pérez-Pariente, Appl. Catal. A 151 (1997) 373.
[110] J. Le Bars, J.C. Védrine, A. Auroux, S. Trautmann, M. Baerns, Appl. Catal. A 119 (1994) 341.
[111] J. Le Bars, J.C. Vedrine, A. Auroux, S. Trautmann, M. Baerns, Appl. Catal. A 88 (1992) 179.
[112] M.S. Faraldos, M.A. Bañares, J.A. Anderson, H. Hu, I.E. Wachs, J.L.G. Fierro, J. Catal. 160 (1996) 214.
[113] M.J. Koranne, J.G. Goodwin Jr., G. Marcelin, J. Catal. 148 (1994) 369.
[114] S.T. Oyama, G.A. Somorjai, J. Phys. Chem. 94 (1990) 5022.
[115] L. Mendelovici, J.H. Lunsford, J. Catal. 94 (1985) 37.
[116] Y. Murakami, K. Otsuka, Y. Wada, Bull. Chem. Soc. Jpn. 63 (1990) 340.
[117] W.-D. Mross, Catal. Rev.-Sci. Eng. 25 (1983) 591.
[118] C. Martín, M.C. Mendizábal, V. Rives, J. Mater. Sci. 27 (1992) 5575.
[119] A. Erdõhelyi, J. Csrényi, F. Solymosi, Catalytic selective oxidation, ACS Symp. Ser. 523 (1993) 368.
[120] A. Erdöhelyi, K. Fodor, F. Solymosi, J. Catal. 166 (1997) 244.
[121] P. Ciambelli, L. Lisi, G. Roouppolo, G. Russo, J.C. Volta, Proceedings of the Third World Congress on Oxidation Catalysis, Stud. Surf. Sci. Catal. 110 (1997) 285.
[122] M. Merzouki, B. Taouk, L. Tessier, E. Bordes, P. Courtine, in: L. Guczi, F. Solymosi, P. Tétényi (Eds.), New Frontiers in Catalysis, Stud. Surf. Sci. Catal. 75 (1993) 1875.
[123] L. Tessier, E. Bordes, M. Gubelmann-Bonneau, Catal. Today 24 (1995) 335.
[124] H.D. Gesser, N.R. Hunter, L.A. Morton, P.S. Yarlagadda, Energy & Fuels 5 (1991) 423.
[125] J. Santamaría-González, M. Martínez-Lara, M.A. Bañares, M.V. Martinez-Huerta, E. Rodríguez-Castellón, J.L.G. Fierro, A. Jiménez-López, J. Catal. 181 (1999) 280.
[126] J. Santamaría-González, M. Martínez-Lara, M.A. Bañares, M.V. Martinez-Huerta, E. Rodríguez-Castellón, J.L.G. Fierro, A. Jiménez-López.
[127] N. Mizuno, M. Misono, Chem. Rev. 98 (1998) 199.
[128] S.S. Hong, J.B. Moffat, Appl. Catal. 109 (1994) 117.
[129] S. Albonetti, F. Cavani, F. Trifirò, M. Koutyrev, Catal. Lett. 30 (1995) 253.
[130] J.B. Moffat, J. Mol. Catal. 26 (1996) 65.
[131] W. Li, W. Ueda, in: R.K. Grasselli, S.T. Oyama, A.M. Gaffney, J.E. Lyons (Eds.), Third World Congress on Selective Oxidation, Stud. Surf. Sci. Catal. 110 (1997) 433.
[132] M. Roy, M. Gubelmann-Bonneau, H. Ponceblanc, J.C. Volta, Catal. Lett. 42 (1996) 93.
[133] P.T. Nguyen, A.W. Sleight, Heterogeneous hydrocarbon oxidation, ACS Symp. Ser. 638 (1996) 236.
[134] Y. Cai, C.B. Wang, I.E. Wachs, in: R.K. Grasselli, S.T. Oyama, A.M. Gaffney, J.E. Lyons (Eds.), Third World Congress on Oxidation Catalysis, Stud. Surf. Sci. Catal. 110 (1997) 255.
[135] G.J. Hutchings, A. Desmartin Chomel, R. Olier, J.C. Volta, Nature 368 (1994) 41.
[136] G.C. Colorio, B. Bonnetot, J.C. Vedrine, A. Auroux, in: V. Cortés Corberán, S. Vic Bellón (Eds.), New Developments in Selective Oxidation, Studs. Surf. Sci. Catal. 82 (1994) 143.
[137] M.A. Bañares, L.J. Alemany, M. López Granados, M. Faraldos, J.L.G. Fierro, Catal. Today 33 (1997) 73.
[138] Y. Uragami, K. Otsuka, Catal. Today 13 (1992) 667.
[139] V. Cortés Corberán, R.X. Valenzuela, B. Sulikowski, M. Derewinski, Z. Oleiniczak, J. Krysciak, Catal. Today 32 (1996) 193.
[140] J.A. Roos, S.J.I. Korf, R.H.J. Veehof, J.G. van Ommen, J.R.H. Ross, Catal. Today 4 (1989) 441–452.
[141] Y. Uragami, K. Otsuka, J. Chem. Soc., Faraday Trans. 88 (1992) 3605.
[142] N.U. Zhanpeison, K. Otsuka, React. Kinet. Catal. Lett. 52 (1994) 27.
[143] E.M. Thorsteinson, T.P. Wilson, F.G. Young, P.H. Kasai, F. Catal. 52 (1978) 116.
[144] R. Burch, R. Swarnakar, Appl. Catal. 70 (1991) 129.
[145] O. Desponds, R.L. Keiski, G.A. Somorjai, Catal. Lett. 19 (1993) 17.
[146] R. Juárez López, N.S. Godjayeva, V. Cortés Corberán, J.L.G. Fierro, E.A. Mamedov, Appl. Catal. A 124 (1995) 281.
[147] E.A. Mamedov, R.M. Tayshinskii, R.G. Rizayez, J.L.G. Fierro, V. Cortés Corberán, Catal. Today 32 (1996) 177.
[148] J.S. Pilgrim, A. McIlroy, G.A. Taatjes, J. Phys. Chem. A 101 (1997) 1873.
[149] R. Burch, G.D. Squire, S.C. Tsang, Appl. Catal. 43 (1988) 105.
[150] R. Burch, E.M. Crabb, G.D. Squire, T.S. Tsang, Catal. Lett. 2 (1989) 249.
[151] R. Burch, S. Chalker, P. Loader, in: L. Guczi, F. Solymosi, P. Tétényi (Eds.), New Frontiers in Catalysis, Stud. Surf. Sci. Catal. 75 (1992) 1079.
[152] S. Sugiyama, K. Sogabe, T. Miyamoto, H. Hayashi, J.B. Moffat, Catal. Lett. 42 (1996) 127.
[153] R.W. Judd, C. Komodromos, T.J. Reynolds, Catal. Today 132 (1992) 237.
[154] R. Burch, S. Chalker, P. Loader, J.M. Thomas, W. Ueda, Appl. Catal A 82 (1992) 77.
[155] S.J. Conway, D.J. Wang, J.H. Lunsford, Appl. Catal. A 79 (1991) L1.
[156] S.J. Korf, J.A. Roos, L.J. Veltman, J.G. van Ommen, J.R.H. Ross, Appl. Catal. 56 (1989) 119.
[157] D. Wang, M.P. Rosynek, J.H. Lunsford, J. Catal. 15 (1995) 155.
[158] D.W. Lewis, R.A. Catlow, Topics Catal. 1 (1994) 111.
[159] W. Ueda, S.W. Lin, I. Tohmoto, Catal. Lett. 44 (1997) 241.
[160] J.Z. Luo, H.L. Wan, Appl. Catal. A 158 (1997) 137.
[161] C.T. Au, K.D. Chen, H.X. daik, Y.W. Liu, J.Z. Luio, C.F. Ng, J. Catal. 179 (1998) 300.
[162] J.A. Roos, S.J. Korf, R.H.J. Veehof, J.G. van Ommen, J.R.H. Ross, Appl. Catal. 52 (1989) 147.
[163] S.J. Conway, J.H. Lunsford, J. Catal. 131 (1991) 513.

[164] H.M. Swaan, A. Toebes, K. Seshan, J.G. van Ommen, J.R.H. Ross, Catal. Today 13 (1992) 629.
[165] A. Argent, P.G. Harrison, J. Chem. Soc., Chem. Commun. (1986) 1058.
[166] E.M. Kennedy, N.W. Cant, Appl. Catal. 75 (1991) 321.
[167] V.T. Amorebieta, A.J. Colussi, J. Am. Chem. Soc. 118 (1996) 10236.
[168] A. Shamsi, Ind. Eng. Chem. Res. 32 (1993) 1877.
[169] M. Loukah, G. Coudirier, J.C. Vedrine, in: P. Ruíz, B. Delmon (Eds.), New Developments in Selective Oxidation by Heterogeneous Catalysts, Stud. Surf. Sci. Catal. 72 (1992) 191.
[170] P. Olivera-Pastor, J. Maza-Rodríguez, A. Jiménez-López, I. Rodríguez-Ramos, A. Guerrero-Ruíz, J.L.G. Fierro, New developments in selective oxidation, in: Second World Congress on Selective Oxidation, Stud. Surf. Sci. Catal. 82 (1993) 103.
[171] S. Pak, E. Smith, M.P. Rosynek, J.H. Lunsford, J. Catal. 165 (1997) 73.
[172] S. Pak, M.P. Rosynek, J.H. Lunsford, J. Phys. Chem. 98 (1994) 11786.
[173] J.H. Lunsford, in: A. Holmen, J.-J. Jens, S. Kolboe, Natural Gas Conversion, Stud. Surf. Sci. Catal. 61 (1990) 3.
[174] S. Hamakawa, K. Sato, K. Takehira, J. Electrochem. Soc. 144 (1997) 1.
[175] K. Otsuka, T. Ando, S. Suprapto, Y. Wand, K. Ebitani, I. Yamanaka, Catal. Today 24 (1995) 315.
[176] N. Djeghri, M. Formenti, F. Juillet, S.J. Teichner, Faraday Disc., Chem. Soc. 58 (1974) 185.
[177] K. Wada, K. Yoshida, Y. Watanabe, T. Suzuki, Appl. Catal. 74 (1991) L1.
[178] K. Marcinkowska, S. Kaliaguine, P.C. Roberge, J. Catal. 90 (1984) 49.
[179] H. Sun, F. Blatter, H. Frei, Catal. Lett. 44 (1997) 247.
[180] V. Blatter, H. Sun, S. Vasenkov, H. Frei, Catal. Today 41 (1997) 297.
[181] K. Wada, K. Yoshida, Y. Watanabe, Appl. Catal. 79 (1991) 143–144.
[182] K. Wada, K. Yoshida, Y. Watanabe, T. Suzuki, J. Chem. Soc., Chem. Commun. (1991) 726.
[183] H. Sun, F. Blatter, H. Frei, Heterogeneous hydrocarbon oxidation, ACS Symp. Ser. 638 (1996) 409.
[184] H. Frei, in: R.K. Graselli, S.T. Oyama, A.M. Gaffney, J.E. Lyons (Eds.), Third World Congress on Oxidation CatalysisStuds, Stud. Surf. Sci. Catal. 110 (1997) 1041.
[185] M. Iwasaki, K. Toriyam, K. Nunome, J. Am. Chem. Soc. 103 (1981) 3591.
[186] J.A.R. Coope, C.L. Gardner, C.A. McDowel, A.I. Pelman, Mol. Phys. 21 (1971) 1043.
[187] A. Sugihara, K. Shimokoshi, I. Yasimori, J. Phys. Chem. 81 (1977) 669.
[188] D. Breck, Zeolite Molecular Sieves: Structure, Chemistry, and Use, Wiley, New York, 1974.
[189] H.D. Gesser, G. Zhu, N.R. Hunter, Catal. Today 24 (1995) 321.
[190] W. Li, S.T. Oyama, Heterogeneous hydrocarbon oxidation, ACS Symp. Ser. 638 (1996) 364.
[191] G.A. Olah, G.K. Surya, P.J. Sommer, Superacids, Chapter 5, Wiley, New York, 1985, p. 243.
[192] G.A. Olah, Y. Halpern, J. Shen, Y.K. Mo, J. Am. Chem. Soc. 95 (1973) 4960.
[193] T.-K. Cheung, B.C. Gates, J. Chem. Soc., Chem. Commun. (1996) 1937.
[194] T.-K. Cheung, B.C. Gates, J. Catal. 168 (1997) 522.
[195] L.D. Schmidt, M. Huff, Catal. Today 21 (1994) 443.
[196] M.C. Huff, L.D. Schmidt, AIChE J. 42 (1996) 3484.
[197] M. Huff, P.M. Torniainen, L.D. Schmidt, Catal. Today 21 (1994) 113.
[198] A.L.Y. Tokovich, J.L. Xilka, D.M. Jimenez, G.L. Roberts, J.L. Cox, Chem. Eng. Sci. 51 (1996) 789.
[199] J. Coronas, M. Menéndez, J. Santamaría, Ind. Eng. Chem. Res. 34 (1995) 4229.
[200] M. Guisnet, N.S. Gnep, F. Alario, Appl. Catal. A 89 (1992) 1.
[201] D. Seddon, Catal. Today 6 (1989) 351.
[202] G. Giannetto, R. Monque, R. Galiasso, Catal. Rev.-Sci. Eng. 36 (1994) 271.
[203] Y. Ono, H. Nakatani, H. Kitagawa, E. Suzuki, in: T. Inui (Ed.), Successful Design of Catalysts, Stud. Surf. Sci. Catal. 44 (1989) 279.
[204] M. Guisnet, N.S. Gnep, D. Aittaleb, J.Y. Doyemet, Appl. Catal. A 87 (1992) 255.
[205] M.S. Scurrel, Appl. Catal. 32 (1987) 1.
[206] S.N. Khadzhiev, L.G. Agabalyan, I.M. Mamaeva, Catal. Today 13 (1992) 635.
[207] P. Chu, Mobil Oil Co., New York, US Patent, 4 120 910 (1978).
[208] M. Guisnet, N.S. Gnep, Appl. Catal. A 146 (1996) 33.
[209] C.J. Norton, Ind. Eng. Chem. Proc. Des. Dev. 3 (1964) 230.
[210] O.V. Bragin, E.S. Shipo, A.V. Prreobrazhenskyu, S.A. Isaev, T.V. Vasina, B.B. Byusenbina, G.V. Antoshin, Kh.M. Minachev, Appl. Catal. 27 (1986) 219.
[211] K.H. Steinberg, U. Mroczek, F. Roessner, Appl. Catal. 66 (1990) 37.
[212] U. Mroxzek, W. Reschetilowski, K. Pietsxh, K.H. Steinberg, React. Kinet. Catal. Lett. 43 (1991) 539.
[213] S. Engels, H. Kausch, B. Matshei, O.V. Bragin, A.V. Preobrazhenskii, T.V. Vasina, Catal. Today 3 (1988) 437.
[214] W. Reschetilowski, U. Mroxzek, K.H. Steinberg, Appl. Catal. 78 (1991) 257.
[215] Y. Ono, Catal. Rev.-Sci. Eng. 34 (1992) 179.
[216] A.W. Chester, Y.F. Chu, Mobil Oil Co., US Patent, 4 350 835 (1982).
[217] L.B. Pierella, G.A. Eimer, O.A. Anunziata, React. Kinet. Catal. Lett. 63 (1998) 271.
[218] F.Y. Chu, A.W. Chester, Mobil Oil Co., US Patent, 4 392 989 (1983).
[219] T. Mole, J.R. Anderson, G. Creer, Appl. Catal. 17 (1985) 141.
[220] J. Bandeira, Y.B. Taarit, Appl. Catal. A 152 (1997) 43.
[221] A. Hagen, O.P. Keipert, F. Roessner, in: J.W. Hightower, W.N. Delgass, E. Iglesia, A.T. Bell (Eds.), 11th International Congress on Catalysis, Stud. Surf. Sci. Catal. 101 (1996) 781.

[222] V.I. Yakerson, T.V. Vasina, L.I. Lafer, V.P. Sytnyk, G.L. Dykh, A.V. Kokhov, O.V. Bragin, H.M. Minachev, Catal. Lett. 3 (1989) 339.
[223] K.M. Dooley, T.F. Guidry, G.K. Price, J. Catal. 157 (1995) 66.
[224] V. Kanazirev, G.L. Price, J.M. Dooley, J. Chem. Soc., Chem. Commun. 9 (1990) 712.
[225] G.L. Price, V. Kanazirev, J.M. Dooley, US Patent, 5 149 679 (1992).
[226] C.T. Chu, S. Han, US Patent, 4 968 650 (1990).
[227] V. Kanazirev, R. Dimitrova, G.L. Price, A.Yu. Khodakov, L.M. Kustov, V.B. Kazanski, J. Mol. Catal 70 (1991) 111.
[228] G.R. Nayense, A.J.H.P. van der Pol, J.H.C. van Hooff, Appl. Catal. 72 (1991) 81.
[229] J. Kanai, N. Kawata, Appl. Catal. 55 (1989) 11.
[230] G.J. Buckles, G.J. Hutchings, J. Catal. 151 (1995) 33.
[231] G.D. Meitzner, E. Iglesia, J.E. Baumgarthner, E.S. Huang, J. Catal. 140 (1993) 209.
[232] O.V. Chetina, T.V. Vasina, V.V. Lunin, O.V. Bragin, Catal. Today 13 (1992) 639.
[233] F. Solymosi, A. Szöke, Appl. Catal. A 166 (1998) 225.
[234] S.T. Wong, Y. Xu, L. Wang, S. Liu, G. Li, M. Xie, X. Guo, Catal. Lett. 38 (1996) 39.
[235] S. Trautmann, M. Baerns, J. Catal. 136 (1992) 613.
[236] A. Pisanu, C.E. Gigola, Appl. Catal. B 11 (1996) L37.
[237] Y. Yu Yao, Ind. Eng. Chem. Prod. Res. Dev. 19 (1980) 293.
[238] R. Burch, P. Loader, F. Urbano, Catal. Today 27 (1996) 24.
[239] Y.-F. Yu Yao, J. Catal. 28 (1973) 139–149.
[240] P.G. Harrison, B. Maunders, J. Chem. Soc., Faraday Trans. 1 81 (1985) 1311.
[241] S. Cheng, S.Y. Cheng, J. Catal. 122 (1990) 1.
[242] E. Finocchio, G. Busca, V. Lorenzelli, R.J. Willey, J. Catal. 151 (1995) 204.
[243] Y.M.L. Ng Lee, Ph.D. Thesis, University Valencia, Spain, 1997.
[244] A. Bielanski, J. Haber, Catal. Rev.-Sci. Eng. 19 (1979) 1.
[245] D. Papageorgiu, A.M. Estathiou, X.E. Verykios, J. Catal. 147 (1994) 279.
[246] A.V. Kucherov, T.N. Kucherova, A.A. Slinkin, Kinet. Catal. 33 (1992) 618.
[247] A.V. Kucherov, C.P. Hubbard, T.N. Kucherova, M. Shelev, Appl. Catal. B 7 (1996) 285.
[248] A.V. Kucherov, T.N. Kucherova, V.D. Nissenbaum, A.A. Slikin, Kinet. Catal. Lett. 36 (1995) 673.
[249] A.V. Kucherov, T.N. Kucherova, A.A. Slinkin, Kinet. Catal. 33 (1992) 877.